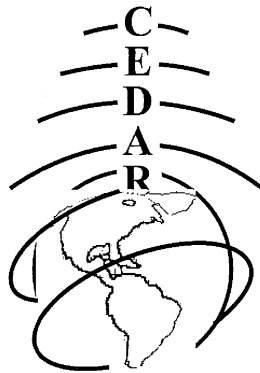


# CEDAR

## 2012

Eldorado Hotel  
Santa Fe, New Mexico



**MLT Poster Session**  
Wednesday June 27, 2012





## **Table of Contents**

### **Instruments and Techniques for the Middle Atmosphere**

|  |   |
|--|---|
| <b>ITMA-01</b> , Andrew John Kavanagh, British Antarctic Survey access to the Middle Atmosphere.....   | 1 |
| <b>ITMA-02</b> , Alireza Mahmoudian, New-Measurement Techniques to Diagnose Charged Dust Clouds in the Near-Earth Space Environment Using Ground-Based Ionospheric Heating Facilities..... | 1 |
| <b>ITMA-03</b> , Mark G. Conde, Scanning Doppler Imager Observations of Two Dimensional Wind and Temperature Fields at Mesopause Heights .....   | 2 |
| <b>ITMA-04</b> , Cody Vaudrin, A Hardware Description of the Colorado Software Defined Radar .....   | 3 |
| <b>ITMA-05</b> , Cody Vaudrin, A Multistatic Common-volume Meteor Wind Radar Measurement Technique .....   | 3 |
| <b>ITMA-06</b> , Stephen Hall, Estimation of Atmospheric Gravity Wave Parameters from Airglow Imagery .....  | 3 |

### **Meteor Science other than Wind Observations**

|  |   |
|--|---|
| <b>METR-01</b> , Alex Fletcher, Simulations of Meteoroid Impact Generated Plasmas .....  | 4 |
| <b>METR-02</b> , Nicolas Lee, Theory and experiments characterizing meteoroid impact plasma dynamics .....                           | 4 |
| <b>METR-03</b> , Vicki Hsu, First Detection of Meteoric Smoke using the Poker Flat Incoherent Scatter Radar.....                     | 4 |
| <b>METR-04</b> , Jonathan Yee, Diffusion of Non-Specular Trails as Measured by ALTAIR .....  | 5 |
| <b>METR-05</b> , Ryan Volz, Radar Waveform Inversion Using Range-Frequency Sparsity.....   | 5 |
| <b>METR-06</b> , Rafael Mesquita, , Statistical Analysis on the Meteor Echoes of CARIRI (7.6° S).....                                | 6 |
| <b>METR-07</b> , Qian Zhu, Modeling Radar Holography as Applied to Point Targets .....   | 6 |
| <b>METR-08</b> , Zachary Stephens, Automated Classification of Meteor Reflections .....  | 6 |
| <b>METR-09</b> , Austin Sousa, Naturally-occurring Low-frequency Radio Emissions during Meteor Showers .....                         | 6 |
| <b>METR-10</b> , Steven Pifko, Modeling the Meteoroid Input Function at Mid-Latitude Using Meteor Observations By the MU Radar ..... | 7 |

### **Mesosphere and Lower Thermosphere Gravity Waves**

|  |   |
|--|---|
| <b>MLTG-01</b> , Laura Angelina Holt, Transport of NO <sub>x</sub> created by energetic particle precipitation in WACCM.....                                   | 7 |
| <b>MLTG-02</b> , Xian Lu, Diurnal variation of gravity wave momentum flux and its forcing on the diurnal tide.....   | 8 |
| <b>MLTG-03</b> , Manja Placke, Investigation of gravity wave momentum fluxes from MF Doppler radar and meteor radar measurements in the polar mesosphere ..... | 8 |
| <b>MLTG-04</b> , Sharon Vadas, Gravity wave ray trace and full wave model: Approximations, assumptions, results, and comparison with observations .....        | 9 |
| <b>MLTG-05</b> , Christopher Heale, Thermospheric Dissipation and Reflection of Upward Propagating Gravity Wave Packets.....                                   | 9 |

|  |    |
|--|----|
| <b>MLTG-06</b> , Geoff Crowley, TID Observations at Middle and Low Latitudes Using the TIDBIT HF TID Mapper .....  | 10 |
| <b>MLTG-07</b> , Ryan Agner, On the Variation of Gravity Wave Activity through the Solar Cycle at the South Pole .....   | 10 |
| <b>MLTG-08</b> , Erin H. Lay, High temporal and spatial-resolution detection of atmospheric gravity wave effects on D-layer electron density .....               | 10 |
| <b>MLTG-09</b> , Neal R. Criddle, Investigating mountain waves in MTM airglow data at Cerro Pachon.....  | 11 |
| <b>MLTG-10</b> , Michael Negale, Short period gravity waves in the Arctic atmosphere over Alaska .....   | 11 |
| <b>MLTG-11</b> , Zhenhua Li, Gravity waves observed by Michelson Interferometer at Sondre Stromfjord, Greenland.....   | 12 |
| <b>MLTG-12</b> , Xuguang Cai, Mesospheric bore study based on USU sodium lidar and Mesospheric Temperature Mapper (MTM) observations in summer 2011 .....        | 12 |
| <b>MLTG-13</b> , Tony Mangogna, 4-Channel Photometer for Gravity Wave Detection and Analysis .....   | 12 |
| <b>MLTG-14</b> , Robert Andrew Marshall, Subionospheric VLF Remote Sensing of Gravity Waves and Acoustic Waves in the Lower Ionosphere .....                     | 13 |
| <b>MLTG-15</b> , Cao Chen, Inertia-gravity waves in Antarctica: A case study with simultaneous lidar and radar measurements at McMurdo (77.8° S, 166.7° E) ..... | 13 |
| <b>MLTG-16</b> , Toru Takahashi, Study on upward propagating atmospheric gravity wave in the polar MLT region using Tromsoe sodium LIDAR.....                    | 14 |

**Mesosphere and Lower Thermosphere Lidar Studies**

|   |    |
|---|----|
| <b>MLTL-01</b> , Zachary Butterfield, Studying the Upper Atmosphere Using a Sodium LIDAR.....   | 14 |
| <b>MLTL-02</b> , Katrina Bossert, Initial Diurnal Sodium Density Observations Over ALOMAR.....  | 15 |
| <b>MLTL-03</b> , Cameron Martus, Sodium and iron resonance lidar observations over Poker Flat Research Range, Chatnika, Alaska (65° N, 147° W) .....      | 15 |
| <b>MLTL-04</b> , Zhibin Yu, Diurnal variations of meteoric Fe layers in the mesosphere and lower thermosphere at McMurdo (77.8S, 166.7E), Antarctica..... | 15 |
| <b>MLTL-05</b> , Wentao Huang, Seasonal variations of the mesospheric Fe layer at McMurdo, Antarctica (77.8°S, 166.7°E) .....                             | 16 |
| <b>MLTL-06</b> , Weichun Fong, Winter Temperature Structures and Variations (30-120 km) at McMurdo Station (77.8°S, 166.7°E) .....                        | 16 |
| <b>MLTL-07</b> , John Westerhoff, Using Power in Rayleigh Lidar for Middle and Upper Atmospheric Studies.....   | 16 |
| <b>MLTL-08</b> , Leda Sox, Upgraded ALO Rayleigh Lidar System and Its Improved Gravity Wave Measurements .....  | 17 |

**Mesosphere or Lower Thermosphere General Studies**

|   |    |
|---|----|
| <b>MLTS-01</b> , Justin D. Yonker, Towards a More Accurate Determination of the N(2D) Yield from the Neutral Dissociation of N2 ..... | 17 |
| <b>MLTS-02</b> , Deepali Vimal Saran, Aeronomical and Spectroscopic Studies of Iron Oxide Emission .....                              | 18 |

|   |    |
|---|----|
| <b>MLTS-03</b> , Cissi Ying-tsen Lin, , The Variations of Nitric Oxide in the Lower Thermosphere Observed by the Remote Atmospheric & Ionospheric Detection System (RAIDS) in Year 2010 ..... | 18 |
| <b>MLTS-04</b> , Richard L. Collins, Turbulence and Wave-Instability in the Arctic Middle Atmosphere.....   | 19 |
| <b>MLTS-05</b> , Richard L. Collins, The Wave-Driven Circulation and Variability of the Arctic Atmosphere.....  | 19 |
| <b>MLTS-06</b> , Brenden Roberts, Structure function analysis of chemical release trails in the mesosphere-lower thermosphere region .....  | 19 |
| <b>MLTS-07</b> , Nate C.M. Bartlett, Laboratory studies of FeO and NiO chemiluminescence .....  | 20 |
| <b>MLTS-08</b> , Michael F. Mitchell, Spread-spectrum VLF remote sensing of ionospheric disturbances.....   | 20 |

### **Mesosphere and Lower Thermosphere Other Tidal or Planetary Waves**

|   |    |
|---|----|
| <b>MLTT-01</b> , Nicholas Pedatella, Simulations of solar and lunar tidal variability in the mesosphere and lower thermosphere during sudden stratosphere warmings and their influence on the low-latitude ionosphere ..... | 21 |
| <b>MLTT-02</b> , Katelynn Greer, Synoptic-Scale Disturbances of the Wintertime Polar Upper Stratosphere and Lower Mesosphere: A Summary of Observed Characteristics & Potential Vorticity Analysis.....                     | 21 |
| <b>MLTT-03</b> , Chiao-Yao She, Counter-intuitive, global dynamical phenomena in the MLT: A qualitative explanation.....  | 22 |
| <b>MLTT-04</b> , Vivien Matthias, Sudden Stratospheric Warming – A composite picture using radar and satellite observations.....  | 22 |
| <b>MLTT-05</b> , Qian Wu, TIEGCM with TIDI lower boundary .....   | 23 |
| <b>MLTT-06</b> , Vu Nguyen, Estimating the Day-to-Day Variability of the Migrating Diurnal Tide Through Satellite Observations .....  | 23 |
| <b>MLTT-07</b> , Fabrizio Sassi, WACCMX nudged by High-Altitude Data Assimilation Products: Early Results During The Northern Hemisphere Winter of 2009 .....   | 24 |

### **Sprites**

|  |    |
|--|----|
| <b>SPRT-01</b> , Caitano L. da Silva, Simulation of leader speeds at gigantic jet altitudes.....   | 24 |
| <b>SPRT-02</b> , Ningyu Liu, Recovery of the lower ionosphere from modifications by negative halos.....  | 24 |
| <b>SPRT-03</b> , Burcu Kosar, Investigation of the density requirement for ionospheric patches for sprite streamer formation at sub-breakdown conditions ..... | 25 |
| <b>SPRT-04</b> , Robert Moore, The dependence of elves on lightning return stroke speed .....  | 25 |
| <b>SPRT-05</b> , Jianqi Qin, Dependence of Positive and Negative Sprite Morphology on Lightning Characteristics and Upper Atmospheric Ambient Conditions.....  | 26 |
| <b>SPRT-06</b> , Xuan-Min Shao, Observations of electron density changes in ionospheric D-layer above tropospheric thunderstorms .....                         | 26 |
| <b>SPRT-07</b> , Samaneh Sadighi, Streamer Discharges from Dielectric Hydrometeors.....  | 26 |

**Stratosphere Studies and Below**

**STRB-01**, Sotirios A. Mallios, of very high potential in intra-cloud lightning in connection with terrestrial gamma ray flashes ..... 27

**STRB-02**, Anthony Teti, A spatially scanning lower and middle atmospheric lidar system in northwest New Jersey..... 28

**STRB-03**, Wei Xu, Source Altitudes of Terrestrial Gamma-Ray Flashes Produced by Stepping Lightning Leaders..... 28

# **CEDAR Workshop – MLT Poster Session Abstracts Day 2 – Wednesday, June 27, 2012**

## **Instruments and Techniques for the Middle Atmosphere**

### **ITMA-01      British Antarctic Survey access to the Middle Atmosphere - by Andrew John Kavanagh**

Status of First Author: Non-student

**Authors:** Andrew J Kavanagh, British Antarctic Survey  
Martin Jarvis, British Antarctic Survey

**Abstract:** The British Antarctic Survey is a leading environmental research centre with a remit to address fundamental questions best answered by studies in the Polar Regions. BAS has a wide-ranging research portfolio which includes atmospheric science ranging from the surface through the middle atmosphere into the geospace region. The Middle Atmosphere Dynamics work-package at BAS uses long-term observations and modelling to determine the global scale dynamical links between the polar middle atmosphere and surface climate. This includes determining how these links are influenced both from above and below. To support this work BAS (sometimes in partnership with other institutions) operates a number of key instruments at its stations at Halley and Rothera, including middle atmosphere radars, airglow imagers, spectrometers and radiosondes. In this poster we provide details of some of the instrumentation available for middle atmosphere research at BAS.

### **ITMA-02      New-Measurement Techniques to Diagnose Charged Dust Clouds in the Near-Earth Space Environment Using Ground-Based Ionospheric Heating Facilities - by Alireza Mahmoudian**

Status of First Author: Student IN poster competition, PhD

**Authors:** A. Mahmoudian and W.A. Scales

**Abstract:** Recently, experimental observations have shown that radar echoes from the irregularity source region associated with mesospheric dusty space plasmas may be modulated by radio wave heating with ground-based ionospheric heating facilities. These experiments show great promise as a diagnostic for the associated dusty plasma in the Near-Earth Space Environment which is believed to have links to global change. The dependency of the backscattered signal strength (i.e. Polar Mesospheric Summer Echoes PMSEs) after the turn-on and turn-off of the radio wave heating on the radar frequency is an unique phenomenon that can shed light on the unresolved issues associated with the basic physics of the natural charged mesospheric dust layer.

The physical process after turn-on and turn-off of radio wave heating is explained by competing ambipolar diffusion and dust charging processes. The threshold radar frequency and dust parameters for the enhancement or suppression of radar echoes after radio wave heating turn-on are investigated for measured mesospheric plasma parameters. It has been shown that predicted enhancement of electron irregularity amplitude after heater turn-on at HF band is the direct manifestation of the dust charging process in the space. Therefore further active experiments of PMSEs should be pursued at HF band to illuminate the fundamental charging physics in the space environment to provide more insight on this unique medium. Preliminary observation results of HF PMSE heating experiment with the new 7.9 MHz radar at the European Incoherent Scatter EISCAT facility appear promising for the existence of PMSE turn-on overshoot.

The first comprehensive analytical model for the temporal evolution of PMSE after heater turn-on is developed and compared to a more accurate computational model as a reference. It is shown that active PMSE heating experiments involving multiple observing frequencies at 7.9 (HF), 56, and 224 MHz (VHF)

may contribute further diagnostic capabilities since the temporal evolution of radar echoes is substantially different for these frequency ranges. It is shown that conducting PMSE active experiments at HF and VHF band simultaneously may allow estimation of the dust density altitude profile, dust charge state variation during the heating cycle, and ratio of electron temperature enhancement in the irregularity source region. These theoretical and computational models are extended to study basic physics of the evolution of relevant dusty plasma instabilities thought to play an important role in irregularity production in mesospheric dust layers. A key focus is the boundary layer of these charged dust clouds. It was shown that for high collision frequencies, the waves may be very weakly excited (or even quenched) and confined to the boundary layer. The excited dust acoustic waves inside the dust cloud with frequency range of 7-15Hz and in the presence of electron bite-outs is consistent with measured low frequency waves near 10 Hz by sounding rocket experiments over the past decade.

Finally, variation of spatial structures of plasma and dust (ice) irregularities in the PMSE source region in the presence of positively charged dust particles is investigated. The correlation and anti-correlation of fluctuations in the electron and ion densities in the background plasma are studied considering the presence of positive dust particle formation. Recent rocket payloads have studied the properties of aerosol particles within the ambient plasma environment in the polar mesopause region and measured the signature of the positively charged particles with number densities of  $(2000 \text{ cm}^{-3})$  for particles of 0.5-1 nm in radius. The measurement of significant numbers of positively charged aerosol particles is unexpected from the standard theory of aerosol charging in plasma. Nucleation on the cluster ions is one of the most probable hypotheses for the positive charge on the smallest particles. The utility being that it may provide a test for determining the presence of positive dust particles. The results of the model described show good agreement with observed rocket data. As an application, the model is also applied to investigate the electron irregularity behavior during radiowave heating assuming the presence of positive dust particles. It is shown that the positive dust produces important changes in the behavior during Polar Mesospheric Summer Echo PMSE heating experiments that can be described by the fluctuation correlation and anti-correlation properties.

### **ITMA-03      Scanning Doppler Imager Observations of Two Dimensional Wind and Temperature Fields at Mesopause Heights - by Mark G. Conde**

Status of First Author: Non-student

**Authors:** M. Conde (mark.conde@gi.alaska.edu)  
M. Singh Dhadly (manbharatsingh@gmail.com)  
C. Anderson (callumenator@gmail.com)  
University of Alaska Fairbanks  
M. G. McHarg (Matthew.Mcharg@usafa.edu)  
US Air Force Academy  
M. Kosch (m.kosch@lancaster.ac.uk)  
Lancaster University

**Abstract:** The Scanning Doppler Imager is an all-sky Fabry-Perot spectrometer that produces high resolution Doppler spectra of a single monochromatic airglow or auroral emission line in many separate fields of view across the sky. It operates by periodically varying (i.e., "scanning") the etalon plate spacing over one interference order, while recording and processing many images of the Fabry-Perot fringe system per scan. Instruments of this type have proven very successful at producing two-dimensional maps of thermospheric wind and temperature fields at E- and F-region heights, based on observations of oxygen emissions at 558 nm and 630 nm respectively. Here we report on the first ever application of this technique to measuring mesopause wind and temperature fields. During the recent 2011-2012 observing season we installed an 843 nm OH filter, on loan from Lancaster University in the UK, into the US Air Force Academy's all-sky imaging Fabry-Perot spectrometer at Gakona in Alaska. The instrument was programmed to include the OH filter in its normal observing cycle -- which also included 558 nm and 630 nm oxygen emissions and, when the aurora was bright, the O+ 732 nm emission as well. The all-sky field of view at 843 nm was resolved into 43 sub-fields, which required integration times of around 10 minutes to achieve good signal/noise ratio spectra. We currently have around 6 months of OH observations,

containing several tens of nights of good data. (The remaining data are not useful, either because of cloud, or because the 843 nm signal was contaminated by leakage of other emissions through the filter when the aurora was bright.) The most interesting geophysical "events" seen in wind and temperature fields so far are nights on which large amplitude quasi-sinusoidal gravity wave perturbations appear simultaneously in both the vertical wind and the divergence of the horizontal wind. Several examples of such events will be presented.

**ITMA-04      A Hardware Description of the Colorado Software Defined Radar**  
- by Cody Vaudrin

Status of First Author: Student NOT in poster competition, Masters

**Authors:** Cody Vaudrin and Prof. Scott Palo, University of Colorado

**Abstract:** A general hardware overview of the Colorado Software Defined Radar (CoSRad). Fundamental hardware specifications are presented along with system topology and applications. A number of measurements from various host MWR systems are presented as a demonstration of the CoSRad measurement capabilities.

**ITMA-05      A Multistatic Common-volume Meteor Wind Radar Measurement**  
**Technique** - by Cody Vaudrin

Status of First Author: Student IN poster competition, Masters

**Authors:** Cody Vaudrin and Prof. Scott Palo, University of Colorado

**Abstract:** A universal software defined data acquisition system brings a number of technical and scientific advances to the field of radar remote sensing. A lack of ground-based instrumentation enabling mesoscale and common-volume, multifrequency studies is identified by the NRC and DASI as a current challenge in providing experimental evidence for various aspects of meteor physics and for continued characterization of the overall geospace environment. Furthermore, CEDAR's strategic vision of 2011 identifies the "development of observational and instrumental strategies for geospace systems studies" as a strategic impetus for the coming decade. With respect to radar remote sensing, these needs are directly addressed with the Colorado Software Defined Radar (CoSRad), a phase synchronous, multistatic and reconfigurable data acquisition system and radar controller. Capable of direct-convert sampling over the VHF band, CoSRad can replace most currently operating VHF radar remote sensing receivers with a well-characterized, common data acquisition and control system. Assorted and sometimes proprietary algorithms used to interpret observations from different systems has historically been a source of measurement uncertainty as is currently the case with JRO's JASMET radar. Additionally, CoSRad has the capability to operate as a universal radar receiver over many radar topologies as demonstrated by the current development of a LFM CW tropospheric boundary layer radar. From a scientific standpoint, CoSRad enables straightforward phase-synchronous, multistatic, multifrequency studies of meteor phenomenology. Common-volume wind measurements enabled by multistatic MWR can remove the assumption of all-sky wind homogeneity thereby increasing spacial resolution. This work aims to reduce uncertainty in VHF radar remote sensing measurements by providing a universal data acquisition and radar control platform in addition to developing the common-volume MWR technique enabled by CoSRad's multistatic phase synchronous capabilities.

**ITMA-06      Estimation of Atmospheric Gravity Wave Parameters from Airglow**  
**Imagery** - by Stephen Hall

Status of First Author: Student IN poster competition, PhD

**Authors:** Stephen Hall, UIUC, hall37@illinois.edu

**Abstract:** Passive observations of airglow emissions provide a simple and affordable method for observation of atmospheric gravity waves. This poster presents a method for estimating horizontal parameters of the gravity waves in a single airglow image through matching with a Gabor filter configured to match a particular wavelength, orientation, and phase. Further, when this analysis is applied to two images representing different times and mean altitudes, estimation of propagation direction, vertical wavelength, and vertical attenuation of the wave becomes possible. This method is demonstrated through analysis of imagery taken at the Andes Lidar Observatory by members of the UIUC Remote Sensing and Space Sciences group.

## **Meteor Science other than Wind Observations**

### **METR-01 Simulations of Meteoroid Impact Generated Plasmas - by Alex Fletcher**

Status of First Author: Student IN poster competition, PhD

**Authors:** Alex Fletcher, Sigrid Close, Stanford University

**Abstract:** We present results from a series of computational simulations of a hypervelocity meteoroid impact on a spacecraft, which can result in electrical damage. A meteoroid impact of sufficient velocity will vaporize and ionize both the projectile and part of the spacecraft, forming plasma that expands into the surrounding vacuum. The simulation is split into two phases. A hydrocode is first used to probe the initial impact, including the propagation of a shock wave in the solid target material and the formation the plasma within the expanding impact crater. The results of these calculations inform the initial conditions for the next phase, a particle-in-cell (PIC) solution for the plasma as it is ballistically expands into the vacuum surrounding the spacecraft. The PIC is a 2D higher order electromagnetic code which uses a discontinuous Galerkin method for the solution of Maxwell's equations. For certain conditions, we observe transverse electromagnetic waves radiating from the expanding plasma at frequencies close to the plasma frequency. This radiation could be the source of numerous electrical failures on spacecraft which have occurred after an impact or during a meteoroid shower. We also compare the simulation results to recent hypervelocity impact experiments performed at a Van de Graaff accelerator.

### **METR-02 Theory and experiments characterizing meteoroid impact plasma dynamics - by Nicolas Lee**

Status of First Author: Student IN poster competition, PhD

**Authors:** Nicolas Lee, Stanford University, nnlee@stanford.edu; Sigrid Close, Stanford University

**Abstract:** Small meteoroids and interplanetary dust particles are common within the solar system and routinely impact larger bodies such as planets and moons. Upon impact on an airless body such as Earth's moon or an asteroid, or on a spacecraft, the impactor's kinetic energy is converted over a very short timescale into energy of vaporization and ionization, resulting in a small, dense plasma. Through ground-based hypervelocity impact tests conducted using a Van de Graaff dust accelerator, we study impacts of small dust particles impacting on different material surfaces at speeds ranging from 1 km/s to 70 km/s. The expansion behavior of the impact plasma is analyzed using measurements from a suite of retarding potential analyzers and direct electrical probes.

### **METR-03 First Detection of Meteoric Smoke using the Poker Flat Incoherent Scatter Radar - by Vicki Hsu**

Status of First Author: Student IN poster competition, PhD

**Authors:** Vicki Hsu, Jonathan T. Fentzke, Christiano Brum, Irina Strelnikova, Markus Rapp, Michael Nicolls

**Abstract:** In this work we present the first results of meteor smoke particles (MSPs) detected in the D-region plasma above the 449 MHz Poker Flat Incoherent Scatter Radar (PFISR) in Alaska (67°N, 149°W). MSPs are believed to be the major source of condensation nuclei for the formation of ice particles, the precursor for Polar Mesospheric Clouds (PMCs) and Polar Mesospheric Summer Echoes (PMSE). In addition, they are thought to contribute to D-region chemistry by providing a surface on which heterogeneous chemistry occurs (Summers and Siskand, 1999). Our results are obtained by utilizing a similar fitting method derived for use at other High Power Large Aperture Radar (HPLA) sites that treats the measured radar signal as the sum of two Lorentzian functions [Strelnikova et al., 2007]. This method allows us to determine particle size distributions and smoke densities (when calibrated electron density data is available) in the range of approximately 70 to 90 km altitude depending on background atmospheric composition. We present results from a period of strong D-Region ionization when the detected signal-to-noise (SNR) from the D-region is strongest (12 - 19 UT). Our results provide insight into the presence and distribution of charged meteoric dust in the polar mesopause region resulting from the condensation of ablated material of meteoric origin.

**METR-04      Diffusion of Non-Specular Trails as Measured by ALTAIR**  
- by Jonathan Yee

Status of First Author: Student IN poster competition, PhD

**Authors:** Sigrid Close, Stanford University

**Abstract:** As a meteoroid enters Earth's atmosphere at velocities greater than 10 km/s, it heats up and ablates due to friction between the meteoroid and the atmosphere. The plasma formed during these events is referred to as heads, the plasma surrounding the meteoroid, and trails, the plasma behind the meteoroid. A particular subset of the trails is non-specular trails, which are thought to be the reflection from field aligned irregularities (FAIs) that form after the onset of turbulence in the meteor trail. Using High Power, Large Aperture (HPLA) Radars, we are able to detect and characterize these meteoroids in the E-region of the ionosphere. The diffusion properties of these meteoroid trails are analyzed using measurements taken by the Advanced Research Project Agency (ARPA) Long-range Tracking and Identification Radar (ALTAIR).

**METR-05      Radar Waveform Inversion Using Range-Frequency Sparsity**  
- by Ryan Volz

Status of First Author: Student IN poster competition, PhD

**Authors:** Ryan Volz, Stanford University, rvolz@stanford.edu  
Sigrid Close, Stanford University

**Abstract:** Signals measured by radar, excluding noise, are derived from two components: the transmitted signal and the target reflectivity. Knowing the transmitted and received signals, the goal is to find the reflectivity, which varies as a function of range and frequency. Without further assumptions, this inverse problem is ill-posed. In practice, it is often assumed that reflection is due to point targets; seeking a filter that gives maximum signal-to-noise ratio (SNR) with this assumption yields the matched filter. However, the matched filter is usually not a true inversion because it often produces sidelobes (spurious signal) at other range-frequency locations. We demonstrate a new point target inversion technique that relies on sparsity and is based on the theory of compressed sensing. Compared to the matched filter, our method gives equivalent results and produces no filtering sidelobes, removes noise, and has a high range and frequency resolution that is not directly constrained by the sampling rate or pulse length. Mismatched or inversion filters also produce no sidelobes, but they do so at a loss of SNR relative to the matched filter. We also give examples of meteor scatter where our method is particularly helpful at addressing open science questions. Though our immediate application is to meteor head echoes, the technique can be applied to any radar target that demonstrates sparsity in range and/or frequency.

**METR-06      Statistical Analysis on the Meteor Echoes of CARIRI (7.6° S)**  
- by Rafael Mesquita

Status of First Author: Student NOT in poster competition, Undergraduate

**Authors:** [1] Rafael Luiz Araújo de Mesquita  
[2] Ricardo Arlen Buriti da Costa  
[3] Amauri Fragoso de Medeiros

**Abstract:** This paper presents a statistical behavior of meteor traces in the equatorial region, more precisely in São João do Cariri (7.6 ° S). We present a description of both spatial and temporal Cariri meteor trails.

**METR-07      Modeling Radar Holography as Applied to Point Targets - by Qian Zhu**

Status of First Author: Student IN poster competition, Masters

**Authors:** Qian Zhu, J. D. Mathews

**Abstract:** The basic mathematical description of radar interferometry is extended to imaging while noting that this just a form of holography. For modeling purposes, this holographic approach is applied to point targets (meteor head-echoes) with different spatial and Doppler trajectories in the case of 5×5 antenna/receiver arrays. The limitations of this approach and standard FFT-based inversion techniques are demonstrated. A maximum entropy approach that yields better results is introduced.

**METR-08      Automated Classification of Meteor Reflections - by Zachary Stephens**

Status of First Author: Student IN poster competition

**Authors:** Zachary Stephens

**Abstract:** The study of meteor flux requires the identification of underdense, overdense, and nonspecular meteor trails, but the large and continuously growing collection of meteor radar data makes event detection and classification by hand impractical. In present work we investigate the usage of Gaussian Mixture Models (GMMs) to automatically identify these reflections. Details concerning detection, feature extraction, and implementation are presented. The classifier was trained and tested on several days worth of data collected from a 50-MHz radar stationed at Fort Macon, North Carolina, in late June 2001.

**METR-09      Naturally-occurring Low-frequency Radio Emissions during Meteor Showers - by Austin Sousa**

Status of First Author: Student NOT in poster competition

**Authors:** Austin Sousa

**Abstract:** In their 2000 paper, "ELF/VLF Radiation Produced by the 1999 Leonid Meteors," Price and Blum documented a correlation between low-frequency radio measurements and optical counts of incident meteors. However, no substantial theory has explained the proposed meteor radio signature. Recently, attempts were made to validate the findings of Price and Blum using data from the Poker Flat Incoherent Scatter Radar and the Stanford VLF database; however, meteor emissions could not be conclusively identified. In August, the VLF group will conduct simultaneous optical and VLF measurements to validate the existence of this phenomenon.

## **METR-10      Modeling the Meteoroid Input Function at Mid-Latitude Using Meteor Observations By the MU Radar - by Steven Pifko**

Status of First Author: Student IN poster competition

**Authors:** Steven Pifko (1), Diego Janches (2), Sigrid Close (1), Jonathan Sparks (3), Takuji Nakamura (4), David Nesvorny (5)

1) Space Environment and Satellite Systems Lab, Department of Aeronautics and Astronautics, Stanford University, Stanford, CA USA

2) Space Weather Lab, Goddard Space Flight Center, NASA, Greenbelt, MD, USA

3) Department of Physics, University of Washington, Seattle, WA, USA

4) National Institute for Polar Research, Tokyo, Japan

5) South West Research Institute, Boulder, CO, USA

**Abstract:** Particles originating outside of Earth orbit are continuously plunging through the upper atmosphere. The vast majority of these particles are sporadic meteoroids, typically the size of a grain of sand, entering the atmosphere at high speeds and depositing a large number of ablated atoms in the Mesosphere and Lower Thermosphere (MLT). Ground-based radar systems are able to detect the ionization created by collisions between a meteoroid and surrounding air molecules (i.e., meteors). Specifically, High Power Large Aperture (HPLA) radar instruments efficiently detect the meteor head echo – an ionized region formed around the meteoroid and moving nearly at the same speed. These observations enable the study of the astronomical origins of meteoroids in addition to the many phenomena in the upper atmosphere that are associated with this incoming flux. The Meteoroid Input Function (MIF) model has been developed with the purpose of understanding the temporal and spatial variability of the meteoroid impact in the atmosphere. This model includes the assessment of potential observational biases, namely the characterization of the particular HPLA radar utilized and its ability to detect particles at a given mass and velocity. The MIF has been shown to accurately predict the meteor detection rate of several HPLA radar systems, including the Arecibo Observatory (AO) and the Poker Flat Incoherent Scatter Radar (PFISR), as well as the seasonal and diurnal variations of the meteor flux at various geographic locations.

In this poster, the MIF model is used to predict several properties of the meteors observed by the Middle and Upper atmosphere (MU) radar, including the distributions of meteor areal density, speed, and radiant location. This study offers new insight into the accuracy of the MIF, as it addresses the ability of the model to predict meteor observations at middle geographic latitudes and for a radar operating frequency in the low VHF band, neither of which has previously been validated for the model. Furthermore, the interferometry capability of the MU radar allows for the previously unavailable assessment of the model's ability to capture information about meteoroid source and speed distributions, which are fundamental inputs into the MIF model. This paper demonstrates that the MIF is applicable to a wide range of HPLA radar instruments and increases the confidence of using the MIF as a global model, and it shows that the model accurately considers the speed and sporadic source distributions for the portion of the meteoroid population observable by MU.

## **Mesosphere and Lower Thermosphere Gravity Waves**

### **MLTG-01      Transport of NO<sub>x</sub> created by energetic particle precipitation in WACCM - by Laura Angelina Holt**

Status of First Author: Student IN poster competition, PhD

**Authors:** Laura A Holt, Cora E Randall, Anne K Smith, Bernd Funke, Gabi Stiller

**Abstract:** Energetic particle precipitation (EPP) creates NO in the mesosphere and lower thermosphere. Observations have shown that this EPP-created NO<sub>x</sub> (EPP-NO<sub>x</sub>) is transported to the stratosphere during the polar night. Simulations from the Whole Atmosphere Community Climate Model (WACCM) also capture this phenomenon, but the amount of EPP-NO<sub>x</sub> transported to the stratosphere is underestimated in

the model compared to observations. In this poster we explore two tunable parameters in WACCM that could potentially address this discrepancy: (1) the amplitude of the gravity wave source spectrum for gravity waves triggered by frontogenesis and (2) the eddy diffusion coefficient. We compare results from several WACCM simulations for the 2005-2006 Arctic winter that are nudged with Modern-Era Retrospective Analysis for Research and Applications (MERRA) data to observations from the Atmospheric Chemistry Experiment (ACE), the Microwave Limb Sounder (MLS) and Sounding of the Atmosphere using Broadband Emission Radiometry (SABER).

**MLTG-02      Diurnal variation of gravity wave momentum flux and its forcing on the diurnal tide - by Xian Lu**

Status of First Author: Non-student, PhD

**Authors:** Xian Lu, lux1@erau.edu, Department of Physical Sciences, Embry-Riddle Aeronautical University

Alan Z. Liu, Department of Physical Sciences, Embry-Riddle Aeronautical University

Steven Franke, Department of Electrical and Computer Engineering, University of Illinois at Urbana-Champaign

**Abstract:** We report for the first time on direct estimations of gravity wave (GW) forcing and its impacts on the diurnal tide (DT) based on meteor radar observations. The 5-year meteor radar wind data obtained at Maui, HI (21N) are composited to derive the momentum fluxes of GWs by applying the Hocking's method [2005], and GW forcings are calculated correspondingly. Significant diurnal variations of the GW momentum flux and its forcing are found, suggesting a strong modulation of the DT on GW momentum flux and GW forcing. The rate of change on the amplitude of the DT due to the GW forcing can reach as large as 100-200 m/s/day locally, whose order is comparable to the Whole Atmosphere Community Climate Model (WACCM) simulation. For the 5-year average, GW forcing tends to enhance the DT in the zonal wind at all altitudes and the meridional wind above 90 km, while it damps the DT in the meridional wind below that. The GW forcing also changes the phase of the DT. It delays the tidal phase at all altitudes in the meridional wind and below 90 km in the zonal wind, while advances the phase above 90 km in the zonal wind. The GW effects on the amplitude of the DT tend to be season-dependent below 90 km for both wind components. It should be noted that the GW effects on the DT are sensitive to their relative phases and thus to the vertical wavelengths of both the DT and the diurnal components of the GW forcings. The 2-year meteor radar wind data collected in Cerro Pachon, Chile (30S) are also used to investigate the GW effects on the DT and the results are compared with Maui.

**MLTG-03      Investigation of gravity wave momentum fluxes from MF Doppler radar and meteor radar measurements in the polar mesosphere - by Manja Placke**

Status of First Author: Student IN poster competition, PhD

**Authors:** Manja Placke, Peter Hoffmann, Markus Rapp, Ralph Latteck

**Abstract:** Gravity waves transport energy and momentum throughout the atmosphere leading to corresponding effects far from their source regions. Due to their exponential amplitude growth with height, gravity waves break and impose their momentum onto the mean flow thereby inducing a force which may even lead to a wind reversal at mesospheric heights. Thus gravity waves have a significant influence on atmospheric circulation patterns. In the present study we will compare gravity wave momentum fluxes derived from the Saura MF radar (69°N, 16°E) and the co-located Andenes meteor radar. With the MF radar narrow beam wind measurements can be performed in the upper mesosphere between about 60 and 100 km. Gravity wave momentum fluxes can be determined from radial velocity variations of coplanar beams when running in the Doppler Beam Steering (DBS) mode by using the method from Vincent and Reid (1983). The meteor radar measures winds from reflections at ionization trails of ablating meteoroids from about 80 to 100 km. A simultaneous determination of momentum fluxes and wind variances is possible by applying a regression method proposed by Hocking (2005). The results for momentum fluxes

of both methods will be discussed. Different selection criteria are used and checked for the calculation of mean vertical profiles and annual variations of these two independent instruments and methods.

**MLTG-04 Gravity wave ray trace and full wave model: Approximations, assumptions, results, and comparison with observations - by Sharon Vadas**

Status of First Author: Non-student

**Authors:** Sharon L. Vadas, NWRA  
Michael Nicolls, SLAC

**Abstract:** We discuss the differences between the author's ray trace model (Vadas and Fritts, 2005, hereafter VF05) and the "Hickey" full wave model (e.g., Walterscheid and Hickey, 2011, hereafter WH11). VF05 finds that a gravity wave (GW)'s vertical wavelength,  $l_z$ , is constant, slightly increases, or decreases in  $z$  above the altitude where a GW's momentum flux is maximum (dubbed  $z_{\text{diss}}$ ), depending on the background parameters. Whereas, the Hickey full wave model predicts that  $l_z$  increases exponentially in  $z$  above  $z_{\text{diss}}$ . This difference appears to arise from the different model assumptions: namely, VF05 assumes that the GW source is time-dependent and spatially localized, whereas the full wave model assumes that the GWs are steady-state and horizontally homogeneous. Next, we examine  $l_z$  data of individual GWs to better understand whether the GWs observed in the thermosphere arise from spatially and temporally-localized sources, or from steady state sources. We present recent and new Arecibo observations.

**MLTG-05 Thermospheric Dissipation and Reflection of Upward Propagating Gravity Wave Packets - by Christopher Heale**

Status of First Author: Student IN poster competition

**Authors:** Heale., C. J  
Snively., J. B  
Hickey., M. P.  
Embry-Riddle Aeronautical University

**Abstract:** Studies of gravity waves in the MLT suggest that the lower thermosphere acts as a barrier to upward energy propagation [e.g., Pitteway and Hines, 1963]. Due to conservation of energy, a wave's amplitude increases as the atmospheric density decreases. However, viscous effects simultaneously increase with decreasing density and counteract the growth of the wave. In the lower thermosphere the viscosity becomes significant enough that dissipation overtakes the growth of the wave and its amplitude will decline.

It has been suggested that the increasing molecular viscosity with altitude may act to shorten the dominant vertical wavelength, resulting in a more horizontal trajectory and a peak altitude of energy and momentum flux occurring in the lower thermosphere. [e.g. Zhang and Yi, 2002; Vadas and Fritts, 2005; Vadas, 2007]. Simultaneously, refraction (and at times reflection) of waves can occur in the thermosphere due to its thermal structure. The lower thermosphere features a dramatic increase in temperature with altitude, due to thermal heating of particles by solar radiation. This large increase in temperature makes it a very stable region of the atmosphere, and thus conducive to the propagation of gravity waves not yet dissipated. Above the lower thermosphere, the temperature structure increases less-rapidly with altitude. This region is less stable, with a longer buoyancy period, and may cause reflection of gravity waves. The nature of wave propagation is further complicated by Doppler shifts due to thermospheric wind flow, which can simultaneously influence propagation paths.

We investigate the propagation of gravity waves into the lower thermosphere using a nonlinear, non-isothermal, and compressible model, which incorporates realistic viscosity and thermal conduction. Case studies are run whereby realistic non-monochromatic packet of gravity waves are excited in the lower

atmosphere by controlled oscillatory sources. These studies examine different parameters effective in controlling the refraction, reflection and maximum altitudes reached by non-breaking gravity wave packets propagating into the thermosphere. Numerical results are compared with predictions made by linear analytical and numerical dispersion relations.

**MLTG-06 TID Observations at Middle and Low Latitudes Using the TIDDBIT HF TID Mapper - by Geoff Crowley**

Status of First Author: Non-student

**Authors:** G. Crowley, A. Reynolds, F. Rodrigues, R. Wilder (ASTRA) gcrowley@astraspace.net  
J. Chau and Otto Castillo (Jicamarca Radio Observatory)

**Abstract:** HF Doppler sounders represent a low-cost and low-maintenance solution for monitoring wave activity in the F-region ionosphere. HF Doppler sounders together with modern data analysis techniques provide both horizontal and vertical TID velocities and wavelengths across the entire spectrum from periods of 1 min to over an hour. ASTRA has developed a new system called "TIDDBIT" (TID Detector Built In Texas), and data will be presented from Doppler sounders in Texas, Virginia, Peru and Antarctica. We show how the TIDDBIT data provides information on wind-filtering of gravity waves. The completeness of the wave information obtained from these systems makes it possible to reconstruct the vertical displacement of isoionic contours over the ~200 km horizontal dimension of the sounder array, which will be demonstrated with movies. The TIDDBIT Sounder was recently deployed in Jicamarca, Peru. Results from the Jicamarca site will be shown and compared with the sounder data from other locations. The TIDDBIT system in Peru detected atmospheric waves generated by the Japanese earthquake/tsunami in March 2011. Spread-F conditions detected by TIDDBIT are also compared with GPS scintillation detected by ASTRA's CASES dual-frequency receiver in Jicamarca. The Pre-Reversal Enhancement in vertical plasma drift causes the F-region ionosphere to rapidly increase in altitude, which is also measured by TIDDBIT in Peru.

**MLTG-07 On the Variation of Gravity Wave Activity through the Solar Cycle at the South Pole - by Ryan Agner**

Status of First Author: Student NOT in poster competition

**Authors:** Ryan Agner

**Abstract:** The sun is the ultimate source of energy for the earth and the primary driver of atmospheric dynamics. The 11-year solar cycle of the sun has had a noticeable effect on the overall climate of the earth in the past. More recent work has seen the diurnal tides being directly influenced by the change in solar energy over the solar cycle at the South Pole. Gravity waves are known to be modulated by solar tides and vice versa so a change in the tides may induce a change in gravity wave parameters. A CCD Spectrometer stationed at the South Pole is used to gather temperatures and brightness's of two separate airglow layers in the upper atmosphere at 87km (OH) and 93km (O2). Two different years are chosen to be analyzed for solar cycle dependencies, 2002 during the previous time of maximum solar activity and 2010 just after the last minimum of solar activity. Time series of temperatures and brightness's are analyzed for gravity waves activity using a lomb-scargle frequency analysis and a least-squares fit with a sine-cosine wave model. Using gravity wave theory and four different detection methods, the vertical and horizontal wavelengths, phase speeds and group velocities are found for these waves during both data gathering seasons. Most wave parameters are found to have an overall increase from 2002 to 2010 with the exception being the derived horizontal wavelengths.

**MLTG-08 High temporal and spatial-resolution detection of atmospheric gravity wave effects on D-layer electron density - by Erin H. Lay**

Status of First Author: Non-student

**Authors:** Erin H Lay (1), Xuan-Min Shao (1), Abram Jacobson (2)

(1) ISR-Division, Los Alamos National Lab

(2) Dept. of Earth and Space Sciences, Univ of WA

elay@lanl.gov

xshao@lanl.gov

abramj@u.washington.edu

**Abstract:** By using lightning signals as probing sources of the D-layer ionosphere, we find evidence that gravity waves are a dominant source of D-layer electron density perturbations on time scales of tens of minutes to hours. Propagating fluctuations in D-layer electron density occur over spatial scales of tens of kilometers. Such variation is detected for a majority of thunderstorm days analyzed. Multi-station analysis for a given large storm shows D-layer perturbations that propagate away from large thunderstorms with a large-scale background propagation toward the east.

The technique that we have developed to make these measurements uses broadband VLF/LF lightning waveforms to measure the ionospheric D-layer near thunderstorms. Variations in the electron density profile itself cause modifications to the time delay and magnitude of a lightning stroke's ionospheric reflection received at a given station. We use these measured parameters (time delay and magnitude) in combination with a VLF/LF frequency-dependent propagation model to retrieve variations in the electron density profile near thunderstorms with high temporal (minutes) and high spatial (tens of kms) resolution.

**MLTG-09      Investigating mountain waves in MTM airglow data at Cerro Pachon**  
- by Neal R. Criddle

Status of First Author: Student IN poster competition, Undergraduate

**Authors:** N. R. Criddle, M. J. Taylor, P.-D. Pautet

**Abstract:** Atmospheric gravity waves have been shown to have important implications for atmospheric dynamics. To better understand the effects of gravity waves on the upper atmosphere Utah State University's Center for Atmospheric and Space Sciences is investigating short period-gravity waves over Cerro Pachon, Chile. As part of collaboration between several universities, USU's contribution is a mesospheric temperature mapper that provides image and temperature data vital to understanding gravity waves at this new mountain site. Mountain waves have been observed on multiple occasions at this site and show clear directional preference as well as seasonal preference. Orographic forcing is thought to be the cause of mountain waves, and wind profiles for select days show that mountain waves may appear in the OH and O<sub>2</sub> airglow layer during periods with stronger winds. Keograms show mountain waves are on average stationary over long periods of time while they can be seen to meander back and forth in the short term.

**MLTG-10      Short period gravity waves in the Arctic atmosphere over Alaska**  
- by Michael Negale

Status of First Author: Student IN poster competition, PhD

**Authors:** M. Negale, M.J. Taylor, K. Nielsen , R.L. Collins

**Abstract:** The propagation nature and sources of short-period gravity waves have been studied extensively at low and mid-latitudes, while their extent and nature at the polar regions are less known. During the last decade, observations from select sites on the Antarctic continent have revealed a significant presence of these waves over the southern Polar Region as well as shown unexpected dynamical behavior. In contrast, observations over the Arctic region are few and the dynamical behavior is unknown. A recent project was initiated in January 2011 to investigate the presence and dynamics of these waves over interior Alaska. This site provides an exceptional opportunity to establish a long-term climatology of short-period gravity waves in the Arctic, including their dominant source regions, influences of large-scale tidal and planetary wave

motion, as well as impact of dominant weather systems such as the polar vortex and Aleutian low. Here we present initial measurements of short-period gravity waves in the Arctic atmosphere over Alaska.

**MLTG-11 Gravity waves observed by Michelson Interferometer at Sondre Stromfjord, Greenland - by Zhenhua LI**

Status of First Author: Non-student, PhD

**Authors:** Zhenhua Li, Gulamabas Sivjee  
Space Physics Research Laboratory,  
Department of Physical Sciences,  
Embry-Riddle Aeronautical University

**Abstract:** OH airglow layer centered at about 87 km provides good proxy for the observation of temperature and density perturbation in the MLT region. Gravity waves play important roles in the middle atmosphere dynamically. Observation of gravity wave statistics in the MLT is important for enhancing our understanding on the MLT dynamics and chemistry. OH 3-1 band rotational temperature and brightness from Michelson Interferometer at Sondre Stromfjord, Greenland (67 N, 51 W) from 1998 to 2012 are derived and analyzed using spectral methods to infer gravity wave propagation characteristics. Wave propagation direction and wave parameters such as horizontal wavelength and wave period are inferred through cross-spectral analysis on time series of temperature and brightness in three azimuths. Due to the time resolution limit (15 minutes interval at each azimuth) and the length of nighttime observation (about 12 hours) the wave periods found are limited to one to five hours. The relationships between gravity wave activity and tides and planetary waves are also examined.

**MLTG-12 Mesospheric bore study based on USU sodium lidar and Mesospheric Temperature Mapper (MTM) observations in summer 2011 - by Xuguang Cai**

Status of First Author: Student IN poster competition, PhD

**Authors:** Xuguang Cai, T. Yuan, P. Dominique, Y. Zhao and M. Taylor,  
Center for Atmospheric and Space Sciences, Utah State University  
xuguang cai : XUGUANG.CAI@aggiemail.usu.edu

**Abstract:** We report the observations of three bore events during 2011 summer captured by USU sodium wind/temperature lidar and Mesospheric Temperature Mapper (MTM) at Logan Utah. In these three bore events, the collaborated observations show that the MLT seems to be preconditioned to some unique temperature and wind structure before the bore appears. To be specific, there existed a cold temperature region formed hours before the bore appeared, sandwiched between warm regions. The same cold region is also accompanied with large vertical wind shear changes. It is also revealed that the bore events caused dramatic changes in temperature and wind fields as it propagates through the mesopause region. In this paper, the lidar and MTM data are used to diagnose the tidal and gravity waves characteristics, as well as momentum flux variations before during the bore events. The TIMED/SABER will also be investigated to provide global temperature structure during these bore events.

**MLTG-13 4-Channel Photometer for Gravity Wave Detection and Analysis - by Tony Mangogna**

Status of First Author: Student NOT in poster competition

**Authors:** Tony Mangogna, mangogni@illinois.edu; Gary Swenson; swenson1@illinois.edu; University of Illinois Urbana-Champaign

**Abstract:** The 4-Channel Photometer measures airglow emissions from OH, O<sub>2</sub>, and O and includes an additional channel for measuring background emissions. Data processing methods will be introduced, along with results from data obtained during January and March of 2012 at the Andes LIDAR Observatory (ALO) located on Cerro Pachon, Chile.

**MLTG-14 Subionospheric VLF Remote Sensing of Gravity Waves and Acoustic Waves in the Lower Ionosphere - by Robert Andrew Marshall**

Status of First Author: Non-student

**Authors:** R. A. Marshall, S. Close, U. Inan

**Abstract:** We present observations of narrowband subionospheric VLF transmitter signals exhibiting coherent fluctuations of 1-2 dB. Spectral analysis shows that the fluctuations have periods of 1.5-5 minutes and are largely coherent. The subionospheric propagation path of the signal from Puerto Rico to Colorado passes over regions of convective and lightning activity, as observed by GOES satellite imagery and NLDN lightning data. We suggest that these fluctuations are evidence of acoustic waves launched by the convective activity below, observed in the 80-90 km altitude range to which nighttime VLF subionospheric remote sensing is most sensitive. Modeling of the VLF transmitter signal propagation shows that these fluctuations are due to a significant vertical displacement of the atmosphere at 85 km altitude. These observations show that VLF-SRS may provide a unique, 24-hour remote sensing technique for acoustic and gravity wave activity.

**MLTG-15 Inertia-gravity waves in Antarctica: A case study with simultaneous lidar and radar measurements at McMurdo (77.8° S, 166.7° E) - by Cao Chen**

Status of First Author: Student IN poster competition, PhD

**Authors:** Cao Chen<sup>1</sup>, Xinzhao Chu<sup>1</sup>, Adrian J. McDonald<sup>2</sup>, Zhibin Yu<sup>1</sup>, Weichun Fong<sup>1</sup>, and Sharon L. Vadas<sup>3</sup>

<sup>1</sup>Cooperative Institute for Research in Environmental Sciences & Department of Aerospace Engineering Sciences, University of Colorado at Boulder, USA

<sup>2</sup>Department of Physics and Astronomy, University of Canterbury, New Zealand

<sup>3</sup> CoRA Division, Northwest Research Associates, Boulder, Colorado, USA.

**Abstract:** A new lidar campaign ongoing at McMurdo (77.8° S, 166.7° E), Antarctica has provided high-resolution temperature data in the mesopause region, which are used to examine gravity waves, along with an existing MF radar co-located at the same station. On 29 June 2011, coherent inertia-gravity wave (IGW) structures were observed in both Fe lidar temperature and MF radar wind. Two dominant waves are observed with wave periods ~7.7 h and ~5.0 h, respectively. The vertical wavelengths for these waves are ~22 and ~23 km, respectively. With simultaneous measurements of temperature and wind, the intrinsic wave properties were determined from hodograph analyses. It is shown that the longer-period wave was propagating toward an azimuth direction of ~11° clockwise from the north with a horizontal wavelength of ~2200 km, and an intrinsic period of ~8 h. The horizontal intrinsic phase speed for this wave is ~76 m/s., and the horizontal and vertical group velocities are calculated to be ~50 m/s and ~0.5 m/s, respectively. The shorter-period wave has an intrinsic period of ~4.5 h and propagates ~100° clockwise from the north with a horizontal wavelength of ~1100 km. The horizontal intrinsic phase speed for this wave is ~68 m/s, and the horizontal and vertical group velocities are calculated to be ~58 m/s and ~1.1 m/s, respectively. Both polarized waves show anti-clockwise rotation direction in hodographs indicating upward propagation of wave energy. But propagation angles very shallow from the horizon (~0.6° for longer-period wave, and ~1.1° for the shorter one), due to the large ratio of horizontal to vertical group velocities. Both IGWs may have originated from geostrophic adjustments of jet streams at different locations around Antarctica.

**MLTG-16 Study on upward propagating atmospheric gravity wave in the polar MLT region using Tromsø sodium LIDAR - by Toru Takahashi**

Status of First Author: Student IN poster competition, PhD

**Authors:** Toru Takahashi(STEL), Satonori Nozawa(STEL), Masaki Tsutsumi(NIPR), Takuo T. Tsuda(NIPR), Takuya D. Kawahara(Shinshu Univ.), Norihito Saito(RIKEN), Shin-ichiro Oyama(STEL), Satoshi Wada(RIKEN), Tetsuya Kawabata(STEL), Hitoshi Fujiwara(Seikei Univ.), Asgeir Brekke(Univ. of Tromsø), Chris Hall(Univ. of Tromsø)

**Abstract:** Atmospheric gravity waves (AGWs) propagating upward from the lower atmosphere dissipate and provide significant amount of energy and momentum flux into the upper mesosphere and the lower thermosphere (MLT). This mechanism plays an important role for general circulation in the whole atmosphere. In previous studies, the observation for AGWs eccentrically-located at middle and low latitudes. Therefore, our knowledge about AGWs in the polar MLT region has not yet reached maturity because of few observations.

Temperature variations measured with a sodium LIDAR installed at Tromsø, Norway (69.6 deg N, 19.2 deg E) showed obvious wavelike structures with downward phase propagation on October 29, 2010 in the height region from 80 to 105 km. Spectral analysis provided oscillation period and vertical wavelength of about 4 hours and 8.8 km, respectively. The amplitude had a peak at 85 km with about 15 K. Of particular interest is temporal variation of the upper limit in the height of wavelike structures. The wavelike structures appeared to propagate up to about 95 km from 1630 UT to 2100 UT, they seemed to propagate to higher level (at least 100 km) from 2100 to 0030 UT. Two candidate mechanisms to produce the temporal development were evaluated: wave dissipation and wind filtering. The temperature in the wave dissipating region increases from the background level, resulting in atmospheric instability, which can be evaluated by Richardson number. The wind filtering process works at which the phase velocity of AGWs is equal to the background wind velocity (this height is called critical layer). AGWs do not propagate further upward beyond the critical layer. The phase velocities of AGWs were derived by hodograph method. Comparison of these two mechanisms from 1700 UT to 2400 UT concluded that wind filtering effect was predominant for this event rather than the wave dissipation process.

Theoretical predication regarding the wind filtering and wave dissipation processes has already proposed. However, we need more observational works to assess the validity of the theory, particularly at high latitudes. This study presented a clear example that LIDAR-derived AGWs are successfully explained by the theory at high latitudes.

**Mesosphere and Lower Thermosphere Lidar Studies**

**MLTL-01 Studying the Upper Atmosphere Using a Sodium LIDAR  
- by Zachary Butterfield**

Status of First Author: Student IN poster competition

**Authors:** Zachary Butterfield (zachtb@comcast.net)  
Titus Yuan (titus.yuan@usu.edu)  
Utah State University

**Abstract:** Studying the mesopause region of the atmosphere (between 80 km and 105 km) is important when trying to understand atmospheric turbulence and global temperature change in the upper atmosphere. A Sodium LIDAR system can be used to generate laser induced fluorescence by Na atoms that are naturally present in this region of the atmosphere. The LIDAR system at Utah State University was designed in such a way that its laser pulses are not only narrow band (120MHz FWHM) but also strictly frequency controlled ( $\pm \sim 1$ MHz), and therefore can measure the profiles of temperature and horizontal wind velocity, as well as sodium density. The mesopause has two distinct levels in its thermal structure and, opposite from intuition, is cold during summer months and warm in the winter. Through the observations of Sodium

LIDAR over the past few decades, a much better understanding of this area of the atmosphere has been gained. However, in order to better understand certain phenomena that occur or to make any reliable inference on climate change more data is needed.

**MLTL-02 Initial Diurnal Sodium Density Observations Over ALOMAR**  
- by Katrina Bossert

Status of First Author: Student IN poster competition, PhD

**Authors:** Katrina Bossert, Bifford Williams, Xinzhao Chu

**Abstract:** Using observations from the sodium lidar system at ALOMAR, Norway (69 N, 16 E), a preliminary look at diurnal trends in density over this arctic region was obtained. The initial data from select months allows for a baseline look at whether there are effects that occur in the arctic during night to day transitions. Analysis of previous density measurements was performed to gain insight into arctic diurnal sodium density changes.

**MLTL-03 Sodium and iron resonance lidar observations over Poker Flat Research Range, Chatnika, Alaska (65° N, 147° W) - by Cameron Martus**

Status of First Author: Student IN poster competition

**Authors:** Cameron M. Martus (cmmartus@alaska.edu), Brita K. Irving, Seth R. Robinson, Richard L. Collins.  
Geophysical Institute and Department of Atmospheric Sciences, University of Alaska Fairbanks, Fairbanks, Alaska, USA .

**Abstract:** Resonance lidar measurements have been ongoing at Poker Flat Research Range (PFRR), Chatnika, Alaska (65°N, 147°W) since 1995. These observations have included measurements of the sodium layer and the iron layer. In addition to the well-understood main layers, we have also documented sporadic high-altitude (~110 km) sodium and iron layers. These layers have rarely been observed and raise questions about the steady-state understanding of the main layers. In this study we present observations of the sporadic layers from PFRR, and discuss their characteristics in terms of current chemical models and anomalies in composition of the background atmosphere. Future resonance lidar studies at PFRR will attempt to enhance our understanding of these layers.

**MLTL-04 Diurnal variations of meteoric Fe layers in the mesosphere and lower thermosphere at McMurdo (77.8S, 166.7E), Antarctica - by Zhibin Yu**

Status of First Author: Student IN poster competition, PhD

**Authors:** Zhibin Yu, Xinzhao Chu, Wentao Huang, Weichun Fong, Brendan R. Roberts

**Abstract:** As one of the main metal species in the mesosphere and lower thermosphere, neutral Fe layers provide an excellent tracer for studying atmospheric dynamics and chemistry. Unfortunately, most Fe measurements were made in the night, except a few reports from the Antarctic and Arctic. So far studies of the diurnal variations of Fe layers are very rare. This situation poses interesting questions like how Fe layers vary through a diurnal cycle, whether such variations change with seasons, and what mechanisms contribute to the diurnal variations. To help address this issue, we report the diurnal variations of Fe densities, based on our lidar observations made at McMurdo, Antarctica. The data were collected with an Fe Boltzmann lidar since late December 2010 through 2011, covering the states of polar days under full sunlight, alternations between day and night, and polar nights under total darkness. By taking composite days, we obtain 24-h Fe coverage for every month, allowing relatively detailed study of the diurnal variations. Our preliminary analyses show an interesting phenomenon that the bottom boundary of Fe layers extends downward from ~80 km to ~75 km or lower when switching from night to day. This

phenomenon is obvious in continuous (straight) 24-h data as well as in composite 24-h data during March and April when the sunlight conditions have day and night switches. The results indicate that photochemistry, rather than wave dynamics, may play an essential role in determining the Fe layer bottom. No obvious diurnal variations are observed in polar summer and mid-winter; however, the layer bottom altitude descends for several kilometers from polar day to polar night. These likely reflect the influences of temperatures, waves, mesospheric clouds and aurora activities.

**MLTL-05      Seasonal variations of the mesospheric Fe layer at McMurdo, Antarctica  
(77.8°S, 166.7°E) - by Wentao Huang**

Status of First Author: Non-student, PhD

**Authors:** Wentao Huang<sup>1</sup>, Xinzhao Chu<sup>1</sup>, Zhibin Yu<sup>1</sup>, Brendan R. Roberts<sup>1</sup>, Weichun Fong<sup>1</sup>, John A. Smith<sup>1</sup>, Chester S. Gardner<sup>2</sup>

<sup>1</sup>Cooperative Institute for Research in Environmental Sciences & Department of Aerospace Engineering Sciences, University of Colorado at Boulder, USA

<sup>2</sup>Department of Electrical and Computer Engineering, University of Illinois at Urbana-Champaign, Urbana, Illinois, USA

**Abstract:** Lidar observations of Fe densities between 70 and 110 km above McMurdo, Antarctica, are used to characterize the seasonal variations of the mesospheric Fe layer near the middle of the Antarctic Circle and the South Pole. Distinct differences are observed comparing to previous results from Rothera (67.5°S, 68.0°W) and the South Pole using the same lidar. The maximum Fe abundance occurs in June at McMurdo, similar to at the South Pole but later than at Rothera (at early May). The Fe peak density peaks in June and September with comparable values at McMurdo. The peak altitude of the Fe layer descends from 93.5 km at the end of December to 84.5 km at the end of September, and then ascends with the progress of the Austral summer. The formation of polar mesospheric cloud (PMC) layers in summer depleted the Fe layer below 89 km and helped push the midsummer Fe layer peak to 93.5 km, which is higher than at both Rothera and the South Pole. The region corresponding to Fe depletion by PMC is higher in altitude than at Rothera and comparable to at the South Pole, and is shorter in period than at the South Pole and comparable to at Rothera. These observations will be modeled by a mesospheric Fe chemistry model driven by a general circulation model and including a detailed micrometeoroid flux and ablation model.

**MLTL-06      Winter Temperature Structures and Variations (30-120 km) at McMurdo  
Station (77.8°S, 166.7°E) - by Weichun Fong**

Status of First Author: Student IN poster competition

**Authors:** Weichun Fong, Xinzhao Chu, Zhibin Yu, Chester S. Gardner, and Cao Chen  
Weichun.fong@colorado.edu

**Abstract:** Over 1000 hours of Fe Boltzmann temperature lidar data have been collected at McMurdo station since 2010. The lidar data provides long-duration continuous observations and diurnal coverage at high latitude. In the MLT region, simultaneous long- and short-period wave activities are observed in almost every observational day in winter time. A coherent wave structure with period between 4 and 6 hours appears in the monthly composite temperature in June. The temperature observation data were compared with existed satellite measurements, such as SABER and OSIRIS, and also the atmospheric model WACCM. We report that WACCM 4.0 is comparable with lidar observation in stratosphere region but is about 20 K colder below mesopause region after gravity wave modification.

**MLTL-07      Using Power in Rayleigh Lidar for Middle and Upper Atmospheric Studies  
- by John Westerhoff**

Status of First Author: Student IN poster competition, PhD

**Authors:** John Westerhoff, University of Illinois, westerho@illinois.edu

**Abstract:** This research project involves the use of power in Rayleigh to extend the altitude capability of a Rayleigh lidar to provide useful measurements above 90 km, where typical Rayleigh lidars cannot provide adequate signal. This experimental lidar system is being developed and tested with the goal of opening up new methods for measuring neutral density and temperature in the mesosphere and lower thermosphere. The specific interest for this system is to measure the amplitudes of atmospheric tides, planetary and gravity wave propagation amplitudes and phase. The use of a high-power, new technology laser and large aperture telescopes allow for power-aperture products of 50-750 Wm<sup>2</sup> with this lidar system, where current systems typically employ 5-10 Wm<sup>2</sup>. The higher power-aperture increases the signal capability of the system, which increases the maximum altitude from which useful measurements can be taken. The use of the latest in photonic sensor technology also maximizes the signal returns for the imager. Simulations of this experimental lidar system show that useful measurements can be taken of the neutral atmosphere up to 120 km. A future observatory using this approach could achieve useful measurements up to 200 km, using a high-power laser and large telescope, such as the 8-meter telescope at Cerro Pachon, Chile.

**MLTL-08      Upgraded ALO Rayleigh Lidar System and Its Improved Gravity Wave Measurements - by Leda Sox**

Status of First Author: Student IN poster competition, PhD

**Authors:** Vincent B. Wickwar<sup>1</sup>, Joshua P. Herron<sup>2</sup>, Marcus J. Bingham<sup>1</sup>, Lance W. Petersen<sup>1</sup> (1Physics and CASS, Utah State University, 2Space Dynamics Lab)

**Abstract:** The Rayleigh-Scatter lidar system at the Atmospheric Lidar Observatory (ALO) on the Utah State campus is currently going through a series of upgrades to significantly improve its observational capabilities. A specific objective of these upgrades is to extend the altitude range over which backscattered photons can be detected. A second objective is to increase the sensitivity of the instrument to be able to analyze the raw data at finer temporal and/or spatial resolutions over the current altitude range. By measuring relative densities, the system will be able to determine absolute temperatures and relative density perturbations, whose variations illustrate gravity wave structures. Gravity wave studies will significantly benefit from the improved system due to the waves' propagation throughout the middle atmosphere and their evolving structures on various spatial and temporal scales during propagation.

**Mesosphere or Lower Thermosphere General Studies**

**MLTS-01      Towards a More Accurate Determination of the N(2D) Yield from the Neutral Dissociation of N<sub>2</sub> - by Justin D. Yonker**

Status of First Author: Student IN poster competition

**Authors:** Justin D. Yonker, Karthik Venkataramani, Scott M. Bailey

**Abstract:** Photoelectron impact dissociation of N<sub>2</sub> to neutral products (PEDN<sub>2</sub>) is one of the principal sources of atomic nitrogen in the lower thermosphere. While the total PEDN<sub>2</sub> cross section is relatively well-known, the branching ratios among the N(4S,2D,2P) are not, with literature values ranging from 0.5 to 0.75 for the net doublet yield. Because doublet N produces NO, while quartet N primarily destroys NO, the unknown yields represent a significant uncertainty in our understanding of thermospheric NO and the properties that NO controls (e.g. E-region ion composition, neutral temperature.)

In contrast to O<sub>2</sub>, the N<sub>2</sub> spectrum is discrete and shows no continuum absorption features characteristic of direct dissociation. Rather dissociation proceeds by excitation to a bound state, followed by predissociation. Due to the absorption of the soft solar x-rays, the photoelectron spectrum hardens as altitude is decreased, with a larger percentage of the PEDN<sub>2</sub> rate coming from the E>100 eV tail. In this high-energy limit, the Bethe approximation allows the individual excitation cross sections to the

predissociating states to be represented by a simple function of the optical oscillator strength (OOS). Assuming the states dissociate to the nearest energetically accessible limit, the recent high-resolution mapping of the N<sub>2</sub> OOS distribution below the N<sub>2</sub> ionization potential enables it to be shown that the PEDN<sub>2</sub> doublet yield is a function of altitude, with the N(2D) channel becoming increasingly dominant in the lower thermosphere. The response of modelled NO to modifications of PEDN<sub>2</sub> is addressed.

**MLTS-02      Aeronomical and Spectroscopic Studies of Iron Oxide Emission**  
- by Deepali Vimal Saran

Status of First Author: Non-student

**Authors:** D.V. Saran<sup>1</sup>, T.G. Slanger<sup>1</sup>, W. Feng<sup>2</sup> and J.M.C. Plane<sup>2</sup>

<sup>1</sup> Molecular Physics Laboratory, SRI International, Menlo Park, CA 94025

<sup>2</sup> School of Chemistry, Faculty of Mathematics and Physical Sciences, University of Leeds, UK

**Abstract:** Iron oxide emission in the terrestrial atmosphere is a new nightglow feature of considerable current interest. Scrutiny of sky spectra from the Echelle Spectrograph and Imager (ESI)/Keck II telescope in Mauna Kea, HI, has revealed the presence of a ubiquitous quasi-continuum between 500 and 700 nm, which has been identified as originating with the excited FeO (FeO\*) molecule [Evans et al., 2010; Saran et al., 2011]. This chemiluminescent emission is generated from the reaction between atomic iron and ozone, and comparison with laboratory spectra involving the reaction of Fe and O<sub>3</sub> [West and Broida, 1975, Burgard et al., 2006], as well as meteor trains [Jenniskens et al., 2000], suggest the atmospheric emission is in fact due to the emitting states of FeO(5Δ). Integrated areas of the FeO\* band profile in the 560-620 nm region with ESI show that the overhead continuum intensity is 3-4 times brighter than the sodium 589 nm lines. Analysis of the temporal variability of this nightglow feature has revealed that there are interesting nighttime variations that are not reflected in the other two ozone-dependent nightglow emitters, the OH 8-2 band and the Na doublet (589 nm). The observations of FeO\* intensity were compared with a 1-dimensional and time-resolved model-FeMOD which describes the iron chemistry in the mesosphere and lower thermosphere (MLT). Implications of our results for studies of the mesosphere and lower thermosphere will be discussed.

DVS is the recipient of an NSF CEDAR postdoctoral fellowship, NSF grant ATM-0924781. TGS was supported by grant ATM-0637433 from NSF Aeronomy. WF and JMCP are supported by NERC grant NE/G019487/1.

References

Burgard, D. A., Abraham, J., Allen, A., Craft, J., Foley, W., Robinson, J., Wells, B., Xu, C., and D. H. Stedman, (2006), *Appl. Spectrosc.* 60, 99-102.

Jenniskens, P., M. Lacey, B.J. Allan, D.E. Self and J.M.C. Plane, (2000), *Earth, Moon and Planets*, 82-83, 429-434.

West, J.B., and H.P. Broida, (1975), *J. Chem. Phys.*, 62, 2566-2574.

Evans, W.F.J., R. L., Gattinger, T.G. Slanger, D.A., Saran, D.V., Degenstein, and E. J. Llewellyn, (2010), *Geophys. Res. Lett.*, 37, L22105.

Saran, D.V., T.G. Slanger, W. Feng and J.M.C. Plane, (2011), *J. Geophys. Res.*, 116, D12303

**MLTS-03      The Variations of Nitric Oxide in the Lower Thermosphere Observed by the Remote Atmospheric & Ionospheric Detection System (RAIDS) in Year 2010** - by Cissi Ying-tsen Lin

Status of First Author: Student IN poster competition, PhD

**Authors:** C. Y. Lin (incen@vt.edu), J. Yonker (yonker@vt.edu), S. M. Bailey (baileys@vt.edu), K. Minschwaner (krm@kestrel.nmt.edu), S. A. Budzien, A. W. Stephan

**Abstract:** Nitric oxide (NO) is a minor constituent of the lower thermosphere though plays numerous key roles there. Its production is very sensitive to those energy sources able to break the strong molecular nitrogen bond; thus, NO concentrations are indicative of energy deposition. Cooling through infrared, NO emission is a crucial part of the thermospheric energy balance. NO is also the terminal ion in the E-region of the ionosphere. If NO is transported to lower altitudes, it is a catalytic destroyer of ozone.

The Remote Atmospheric and Ionospheric Detection System (RAIDS) is a suite of limb viewing radiance monitors observing the lower thermosphere at wavelengths from the EUV through the NIR. An inverse technique is applied to radiance profiles near 237 nm so that the vertical profile of NO density can be determined. RAIDS is the only experiment for several decades that observed NO profiles at all daytime local times. Thus, it observes the temperature driven diurnal and seasonal variations in NO. In this study, we show the variations of nitric oxide in the lower thermosphere (100 – 150 km) observed by RAIDS throughout the year 2010. The main focus is put onto the variation of NO with local sunlit time.

**MLTS-04      Turbulence and Wave-Instability in the Arctic Middle Atmosphere**  
- by Richard L. Collins

Status of First Author: Non-student

**Authors:** Richard L. Collins, Brita K. Irving, Aroh Barjatya, Gerald A. Lehmacher

**Abstract:** Measurements of turbulence in the middle atmosphere and upper atmosphere have yielded a wide range of values of energy dissipation rates that vary by several orders of magnitude over small intervals that indicate strong layering of the turbulence and/or the atmospheric stability. This variability complicates the interpretation of the turbulence in terms of energy dissipation and eddy diffusion and makes application of the observations to current general circulation models. Studies to-date indicate that the western Arctic may be a center of action for planetary wave breaking and formation of persistent mesospheric inversion layers due to the presence of the Aleutian anticyclone and the interactions between the anticyclone and the Arctic vortex during periods of enhanced planetary wave activity. We review turbulence measurements in the mesosphere and lower thermosphere and present experimental strategy for studying turbulence in the presence of persistent instabilities in the upper mesosphere and lower thermosphere.

**MLTS-05      The Wave-Driven Circulation and Variability of the Arctic Atmosphere**  
- by Richard L. Collins

Status of First Author: Non-student

**Authors:** Richard L. Collins, Amal Chandran, Brita K. Irving, Seth R. Robinson, Matthew J. Titus, V. Lynn Harvey

**Abstract:** We present observations, reanalyses and model simulations that are being used to understand the interactions between planetary waves, gravity waves and the general circulation in the polar middle atmosphere. Our study is focused on the Arctic stratosphere and mesosphere in winter, when the general circulation is disrupted by sudden stratospheric warming (SSW) events. During these events the zonal winds, latitudinal temperature gradients, and residual circulation of the middle atmosphere are reversed. These events offer the opportunity to understand wave driving of the general circulation. We highlight observations from the 2011-12 winter when a SSW occurred.

**MLTS-06      Structure function analysis of chemical release trails in the mesosphere-lower thermosphere region** - by Brenden Roberts

Status of First Author: Student IN poster competition

**Authors:** B. Roberts and M. F. Larsen  
Dept. of Physics & Astronomy  
Clemson University  
Clemson, SC, USA

**Abstract:** The transition in the turbulent dynamical processes across the turbopause in the mesosphere–lower thermosphere (MLT) region are still poorly understood, in part because of the scarcity of direct observations of the processes. Trimethyl aluminum (TMA) trails released from sounding rockets in that altitude range are often visible for periods in excess of several tens of minutes. An analysis of the structure function for a trail released from a launch in Alaska in 2007 by Wanliss and Larsen (2010) showed a transition from Navier-Stokes turbulence, to three-dimensional turbulence, and then eventually to two-dimensional turbulence as the horizontal scale of the trail grew from approximately 1 km to approximately 100 km. Now, similar analyses of trails from other sounding rocket launches between 2004–2009 confirm this result. The transition to two-dimensional turbulence implies that a reverse cascade can operate in which mean flow, and thus rapid large-scale transport, can be supported by the turbulent processes.

**MLTS-07      Laboratory studies of FeO and NiO chemiluminescence**  
- by Nate C.M. Bartlett

Status of First Author: Non-student, PhD

**Authors:** Nate C.M. Bartlett, Konstantinos Kalogerakis, Richard A. Copeland and Tom G. Slanger

**Abstract:** Although the terrestrial nightglow spectrum has been studied for over a century new identifications continue to be made. Recently, FeO\* continuum emissions in the mesosphere were identified by the comparison of results from the OSIRIS spectrometer to existing laboratory spectra. This discovery has sparked a renewal of interest in the reactions of meteoric metals with mesospheric gases,<sup>2,3</sup> and has motivated the current study. We report laboratory-based chemiluminescence spectra from the reactions

Fe + O<sub>3</sub> and Ni + O<sub>3</sub> produced under various conditions. Iron and nickel vapor was prepared in a vacuum cell using laser ablation at 248 and 800 nm in the presence of ozone. Emission spectra from FeO\* and NiO\* were recorded in the region of 450–700 nm using a commercial fiber-coupled spectrometer and are compared to previous results using different methods.

Support from the NSF Aeronomy Program under grant AGS-0637433 is gratefully acknowledged.

References

1. W.F.J. Evans, R.L. Gattinger, T.G. Slanger, D.V. Saran, D.A. Degenstein, and E.J. Llewellyn, *Geophysical Research Letters*, 37, L22105, (2010).
2. D.V. Saran, T.G. Slanger, W. Feng, and J.M.C. Plane, *Journal of Geophysical Research*, 116, D12303, (2011).
3. R.L. Gattinger, W.F.J. Evans, and E.J. Llewellyn, *Canadian Journal of Physics*, 89, 869, (2011).

**MLTS-08      Spread-spectrum VLF remote sensing of ionospheric disturbances**  
- by Michael F. Mitchell

Status of First Author: Student IN poster competition, PhD

**Authors:** Michael F. Mitchell  
University of Florida  
mmitchell.ufl@gmail.com  
Robert C. Moore  
University of Florida  
moore@ece.ufl.edu

**Abstract:** A new spread-spectrum VLF remote sensing technique is applied to early/fast and lightning-induced electron precipitation (LEP) events. We demonstrate that the scattered fields observed during LEP events exhibit a strong dependence on frequency, whereas those observed during early/fast events do not.

## **Mesosphere and Lower Thermosphere Other Tidal or Planetary Waves**

### **MLTT-01 Simulations of solar and lunar tidal variability in the mesosphere and lower thermosphere during sudden stratosphere warmings and their influence on the low-latitude ionosphere - by Nicholas Pedatella**

Status of First Author: Non-student

**Authors:** Nicholas Pedatella (NCAR/HAO)  
Hanli Liu (NCAR/HAO)  
Arthur Richmond (NCAR/HAO)  
Astrid Maute (NCAR/HAO)  
Tzu-Wei Fang (NOAA/CIRES)

**Abstract:** Whole Atmosphere Community Climate Model (WACCM) simulations are used to investigate solar and lunar tide changes in the mesosphere and lower thermosphere (MLT) that occur in response to sudden stratosphere warmings (SSWs). The average tidal response is demonstrated based on 23 moderate to strong Northern Hemisphere SSWs. The migrating semidiurnal lunar tide is enhanced globally during SSWs, with the largest enhancements (~60-70%) occurring at mid to high latitudes in the Northern Hemisphere. Enhancements in the migrating solar semidiurnal tide (SW2) also occur up to an altitude of 120 km. Above this altitude, the SW2 decreases in response to SSWs. The SW2 enhancements are 40-50%, making them smaller in a relative sense than the enhancements in the migrating semidiurnal lunar tide. Changes in nonmigrating solar tides are, on average, generally small and the only nonmigrating tides that exhibit changes greater than 20% are the diurnal tide with zonal wavenumber 0 (D0) and the westward propagating semidiurnal tide with zonal wavenumber 1 (SW1). D0 is decreased by ~20-30% at low latitudes, while SW1 exhibits a similar magnitude enhancement at mid to high latitudes in both hemispheres. The tidal changes are attributed to a combination of changes in the zonal mean zonal winds, changes in ozone forcing of the SW2, and nonlinear planetary wave-tide interactions. We further investigate the influence of the lunar tide enhancements on generating perturbations in the low latitude ionosphere during SSWs by using the WACCM-X thermosphere to drive an ionosphere-electrodynamics model. For both solar maximum and solar minimum simulations, the changes in the equatorial vertical plasma drift velocity are similar to observations when the lunar tide is included in the simulations. However, when the lunar tide is removed from the simulations, the low latitude ionosphere response to SSWs is unclear and the characteristic behavior of the low latitude ionosphere perturbations that is seen in observations is no longer apparent. Our results thus indicate the importance of variability in the lunar tide during SSWs, especially for the coupling between SSWs and perturbations in the low latitude ionosphere.

### **MLTT-02 Synoptic-Scale Disturbances of the Wintertime Polar Upper Stratosphere and Lower Mesosphere: A Summary of Observed Characteristics & Potential Vorticity Analysis - by Katelynn Greer**

Status of First Author: Student IN poster competition, PhD

**Authors:** Katelynn Greer- CU Aerospace  
Jeffrey Thayer- CU Aerospace  
V. Lynn Harvey- CU LASP  
Hani Liu- NCAR HAO  
Ethan Peck- CU Atmospheric Science  
Cora Randall- CU Atmospheric Science LASP

**Abstract:** Throughout the winter season the polar middle atmosphere is intermittently disturbed; the most spectacular type of disturbance is a major Sudden Stratospheric Warming (SSW). However, the region is dynamically active and exhibits other types of related disturbances on a more frequent, intraseasonal basis. One such disturbance is synoptic-scale “weather events” observed in lidar and rocket soundings, soundings from the TIMED/SABER instrument and UK Meteorological Office (MetO) assimilated data. These disturbances are most easily identified near 42 km where temperatures are elevated over baseline conditions by 50 K and an associated cooling is observed near 75 km. As these disturbances have a vertical structure extending into the lower mesosphere, they will be termed Upper Stratospheric/Lower Mesospheric (USLM) disturbances.

We investigate the dynamical mechanisms responsible for USLM disturbances using the above mentioned observations in addition to model outputs from the Whole Atmosphere Community Climate Model (WACCM4). Results indicate that WACCM reliably reproduces USLM disturbances in terms of thermal structure, the seasonal distribution of events, and temperature profiles through the warm temperature anomaly (peaks at 2 hPa with temperatures in excess of 300 K). Both WACCM and MetO illustrate a clear preference for the temperature anomaly to be located on the East side of the polar vortex (which is distorted and displaced off the pole). Onset of USLM disturbance appears to be related to planetary wave amplification several days in advance. Potential vorticity analysis (including the Charney-Stern criteria for instability and the role of baroclinic/barotropic instabilities) is used to elucidate the dynamics in the development of USLM events. Employing EP-flux as a complementary analysis technique, the role instability plays is demonstrated in its interaction with the zonal mean flow and the conversion of potential energy to kinetic energy. In addition, USLM disturbances appear to have front-like behavior analogous to the troposphere. Broader impacts of these disturbances and the dynamics associated with them influence gravity wave generation/propagation, vertical air motion and chemical tracer transport.

**MLTT-03      Counter-intuitive, global dynamical phenomena in the MLT: A qualitative explanation** - by Chiao-Yao She

Status of First Author: Non-student

**Authors:** Chiao-Yao (Joe) She, Emeritus, Physics Department, Colorado State University, joeshe@lamar.colostate.edu  
Tao Li, Department of Geophysics and Planetary Science, University of Science and Technology of China, Hefei, Anhui, China  
Tao (Titus) Yuan, CASS, Physics Department, Utah State University

**Abstract:** In this pedagogical poster, we explain the climatology of atmospheric state, and the influence of SSW (Sudden Stratospheric Warming) and ENSO (El Niño Southern Oscillation) in the winter mesosphere and lower thermosphere (MLT), all from appropriate balance between Coriolis force and the body force resulting from wave breaking (either gravity wave or planetary wave). Though it took us considerable learning and thinking to appreciate these giant, interesting, and counter-intuitive phenomena and applied them to understand years of Na lidar data we acquired, that they can be understood coherently and simply, we think, is intriguing and encouraging. As a pedagogical poster, we particularly welcome the visit of beginning students as they are preparing to take on the exciting MLT sciences. We also welcome experts in the field; their visits will help to ensure the correctness of our qualitative accounts and improve the “hand-waving” explanation present that will be presented.

**MLTT-04      Sudden Stratospheric Warming – A composite picture using radar and satellite observations** - by Vivien Matthias

Status of First Author: Student IN poster competition, PhD

**Authors:** Peter Hoffmann, hoffmann@iap-kborn.de  
Markus Rapp, rapp@iap-kborn.de  
Gerd Baumgarten, baumgarten@iap-kborn.de

**Abstract:** The winter atmosphere at mid and polar latitudes is disrupted by the most prominent vertical coupling process - the Sudden Stratospheric Warming (SSW). This strong variability occurs due to enhanced planetary wave activity interacting with background winds, gravity waves and tides. The strength and locality of a warming differs from year to year.

By combining global satellite measurements with high resolution radar observations at Andenes (69°N,16°E) and Juliusruh (54°N,13°E) the characteristics of SSWs in the stratosphere and mesosphere are investigated.

Composite pictures of wind and waves of major SSWs show an earlier onset of the wind reversal in the mesosphere than in the stratosphere and a superposition of an oscillation and a westward propagating planetary wave 1 with periods of 10 and 16 days before and during the SSW. Other waves of interest are gravity waves and tides.

### **MLTT-05 TIEGCM with TIDI lower boundary - by Qian Wu**

Status of First Author: Non-student

**Authors:** Qian Wu, HAO/NCAR  
Dave Ortland NWRA

**Abstract:** TIEGCM is a community model NCAR HAO developed. In the past the model is driven at the 95 km lower boundary by GSWM tides. Recently, a self-consistent lower boundary based on TIMED TIDI and SABER observation has been developed. The new lower boundary condition offers not only seasonal variations, but also inter-annual variations. Both migrating and nonmigrating tides are included. Hence the new lower boundary condition is ideal tool for investigating inter-annual variations in the thermosphere originated from the MLT region. Simulation with the new boundary condition has shown clear upward propagation of diurnal eastward propagating zonal wavenumber 3 tide (DE3). Because TIEGCM has electrodynamics in the model, the thermospheric simulation of the nonmigrating tide will be more realistic by including ion drag effect. Simulations based on the new boundary condition are available for community use.

### **MLTT-06 Estimating the Day-to-Day Variability of the Migrating Diurnal Tide Through Satellite Observations - by Vu Nguyen**

Status of First Author: Student IN poster competition, PhD

**Authors:** Vu Nguyen

**Abstract:** The project introduces a novel method to estimate the short term variability of the migrating diurnal tide on a global scale. The method employs data from two satellite instruments, the MLS (Microwave Limb Sounder) instrument on the EOS (Earth Observing System) Aura spacecraft and the SABER (Sounding of the Atmosphere using Broadband Emission Radiometry) instrument on the TIMED (Thermosphere Ionosphere Mesosphere Energetics and Dynamics) spacecraft, in order to acquire measurements at four daily solar local times. As a result, a least squares fit representing the migrating diurnal tide can be constructed, and the daily zonal mean, migrating diurnal amplitude and migrating diurnal phase are all estimated on a daily basis. To produce accurate estimates of the migrating diurnal tide, the error from several sources is reduced. Instrument biases, revealed through a comparative analysis, are first removed. Non-migrating effects are attenuated by zonal averaging, while the errors introduced by other migrating tides are reduced if the solar local time sampling is evenly spaced. The sampling of solar local time, which changes over time due to orbit of the TIMED satellite, displays a large influence on the results as poor sampling causes nearly linearly-dependent solutions. Consequently, the quality of the estimates for the diurnal amplitude and phase varies over time and geographic location. Comparison to theory and past observation indicate that estimates are sufficient for scientific analysis near the equatorial-

mesosphere where the solar local time sampling is well-spaced, the amplitude of the migrating diurnal tide is large, and the amplitudes of other tides and waves are small.

**MLTT-07      WACCMX nudged by High-Altitude Data Assimilation Products: Early Results During The Northern Hemisphere Winter of 2009**

- by Fabrizio Sassi

Status of First Author: Non-student

**Authors:** J. Ma, H.-L. Liu, L. Coy, J. Emmert

**Abstract:** We present early results from a numerical simulation that exercises a version of the Whole Atmosphere Community Climate Model – eXtended version (WACCMX) nudged toward data assimilation products that extend from the ground to the upper mesosphere (~92 km). The data assimilation products are a hybrid data set that includes atmospheric specification from NASA/MERRA and the NRL’s NOGAPS-ALPHA data assimilation systems. The model is constrained up to ~92 km, and is free running above that altitude. We focus on the early months of 2009 to show the impact on the dynamics and composition of the thermosphere from a major stratospheric warming in late January 2009. The overall dynamical behavior, while consistent with other published results, shows a richer and more complex behavior: 2-day wave, ultra-fast Kelvin waves, migrating and non-migrating tides, along with travelling planetary scale normal modes are shown to appear prominently in the lower thermosphere. We attempt to explain the tidal modifications with the influence of dynamical behavior emerging from the lower atmosphere.

**Sprites**

**SPRT-01      Simulation of leader speeds at gigantic jet altitudes - by Caitano L. da Silva**

Status of First Author: Student IN poster competition, PhD

**Authors:** Caitano L. da Silva and Victor P. Pasko, Communications and Space Sciences Laboratory, Department of Electrical Engineering, Pennsylvania State University

**Abstract:** Lightning leaders advance in space by creating a heating conversion zone in their tips (i.e., streamer-to-leader transition) in which Joule heating produced by currents of many non-thermal corona streamers transform into a hot and conducting leader channel. It is believed that the initial stages of transient luminous events termed Gigantic Jets (GJs) propagating toward the lower ionosphere are directly related to leaders initiated by conventional intra-cloud lightning discharges and escaping upward from thundercloud tops. In the present work we provide quantitative description of speeds of these leaders as a function of leader current and ambient air density (altitude). The direct comparisons with available experimental data indicate that the initial speeds of GJs of ~50 km/s are consistent with leaders possessing currents 2-8 A. The observed acceleration of GJs can be explained by growth of the leader current, and at high altitudes (low air densities) may be significantly affected by predominance of non-thermal (i.e., streamer) discharge forms.

**SPRT-02      Recovery of the lower ionosphere from modifications by negative halos**

- by Ningyu Liu

Status of First Author: Non-student

**Authors:** Ningyu Liu (nliu@fit.edu)

Department of Physics and Space Sciences, Florida Institute of Technology, Melbourne, FL, USA.

**Abstract:** We recently reported a modeling study on sprite halos caused by positive cloud-to-ground (CG) lightning flashes using a fluid model that takes into account multiple ion species and electron detachment process of O<sup>-</sup> ions [Liu, JGR, 117, A03308, 2012]. The modeling results indicate that the electron

detachment from O<sup>-</sup> ions allows electron density to grow even at the sub-breakdown condition (i.e., the lightning field is smaller the breakdown threshold field) and the sprite halo front can descend to a lower altitude than previously thought, which can be important for initiation of sprite streamers at 60-75 km altitudes.

In this talk, we will present the results of applying the same model to study the dynamics of sprite halos caused by negative CG. It will focus on the modification of the ionosphere by the halo. For halos caused by positive CG, their fronts typically become very sharp as they descend downward, so simulations may suffer from numerical instability eventually [Liu, 2012]. However, the front of a negative halo caused by lightning of similar strength is smoother, and the model can simulate the entire lifetime of the ionospheric disturbances from the creation to disappearance. We will show the ionospheric perturbations created by the negative halo and discuss how the ionosphere recovers to its original state.

### **SPRT-03      Investigation of the density requirement for ionospheric patches for sprite streamer formation at sub-breakdown conditions - by Burcu Kosar**

Status of First Author: Student IN poster competition, PhD

**Authors:** Burcu Kosar (bkosar@my.fit.edu)  
Dr. Ningyu Liu (nliu@fit.edu)  
Dr. Hamid K. Rassoul (rassoul@fit.edu)

**Abstract:** Sprites are large scale natural plasma phenomena occurring due to penetration of quasi-electrostatic lightning field to mesospheric/lower ionospheric altitudes [Pasko, JGR, 115, 2010]. Sprites consist of filamentary plasma channels known as streamers that are highly non-linear and self-organized ionization waves. Recent high-speed observations of sprites and electromagnetic measurements of lightning electric fields found that sprites often form in lightning fields below the conventional breakdown threshold field  $E_k$  [Hu et al., JGR, 112, 2007; Li et al., JGR, 113, 2008]. The current sprite theory can not offer a satisfactory explanation for these observational results, since it requires the lightning field to exceed  $E_k$  in the lower ionosphere to trigger sprites.

Recently, we have found a possible physical mechanism to initiate sprites at sub-breakdown conditions that is sprite streamers can be successfully initiated from ionospheric patches in a lightning field below  $E_k$  [Kosar et al., JGR, in review]. The origin of those ionization patches may be attributed to ionospheric disturbances created by meteor trails, electrodynamic effects from thunderstorm and/or lightning, and gravity wave breaking [e.g., Suszcynsky et al., GRL, 104, 1999; Stenbaek-Nielsen et al., GRL, 27, 2000; Zabolin and Wright, GRL, 28, 2001; Sentman et al., JASTP, 65, 2003 ; Mende et al., JGR, 110, 2005]. It was also found that the density of the ionization patch is a critical parameter determining whether the streamer can be formed or not. The required peak density of the patch is a couple of orders of magnitude higher than the ambient density at lower ionospheric altitudes. In this talk, we discuss the possibility of lowering the density requirement for the ionization patch and report simulation results for streamer formation at sub-breakdown conditions from the patch with lower densities. We also report simulation results for streamer formation and propagation in the presence of an ambient electron density and discuss its effects on streamer characteristics. Finally, we examine the likely origins for those patches and estimate their lifetimes once they are created in the upper atmosphere.

### **SPRT-04      The dependence of elves on lightning return stroke speed - by Robert Moore**

Status of First Author: Non-student

**Authors:** Robert C. Moore  
University of Florida  
moore@ece.ufl.edu

**Abstract:** A numerical model for the generation of elves is evaluated for a variety of lightning return stroke speeds. We show that the lightning return stroke speed is an important factor in the generation of elves and we present the numerical modeling results.

**SPRT-05      Dependence of Positive and Negative Sprite Morphology on Lightning Characteristics and Upper Atmospheric Ambient Conditions - by Jianqi Qin**

Status of First Author: Student IN poster competition, PhD

**Authors:** Jianqi Qin, Sebastien Celestin, Victor P. Pasko

**Abstract:** Carrot sprites, exhibiting both upward and downward propagating streamers, and columniform sprites, characterized by predominantly vertical downward streamers, represent two distinct morphological classes of lightning driven transient luminous events in the upper atmosphere. In the present work, a two-dimensional plasma fluid model is applied in framework of a two-step technique, in which we couple the large-scale halo dynamics and development of small-scale streamers [Qin et al., GRL, 39, L05810, 2012]. The modeling is used to simulate sprite-halo events over a timescale of 5 ms in order to study the dependence of sprite morphology on lightning characteristics and upper atmospheric ambient conditions. The most significant associative detachment process  $O+N_2 \rightarrow e+N_2O$  in sprite chemistry has been taken into account. It is found that lightning characteristics, namely the total charge moment change, the impulsiveness of the initial lightning pulse, continuing current, and lightning polarity, have significant impact on sprite morphology. For example, it is found that columniform sprites are produced in sub-breakdown conditions, and that continuing current is of essential importance to the development of the upper diffuse region of carrot sprites. Most interestingly, negative sprites are necessarily carrot sprites produced by large charge moment changes. We also find different charge moment change thresholds for the production of positive and negative sprites, which are 320 C km and 500 C km, respectively, under typical nighttime conditions assumed in this study. This difference represents one of the major factors in the polarity asymmetry between +CGs and -CGs in producing sprite streamers. We further demonstrate that lower ambient conductivity leads to smaller threshold charge moment changes required for the production of carrot sprites.

**SPRT-06      Observations of electron density changes in ionospheric D-layer above tropospheric thunderstorms - by Xuan-Min Shao**

Status of First Author: Non-student

**Authors:** Xuan-Min Shao, Erin H. Lay, Abram R. Jacobson

**Abstract:** By using time-domain lightning return stroke waveforms detected remotely from the parental thunderstorms and by comparing the waveform features with ground/ionosphere propagation prediction, electron density profile for the ionospheric D-layer can be retrieved. The signatures of the reflected signal (time delay and amplitude) are directly related to the profile of the electron density. Focusing on the first-hop reflection, each stroke will probe a small area at the mid-point between the stroke and the receiver, and therefore a high spatial resolution detection of the D-layer profile can be obtained.

In this presentation, we report observations above two thunderstorms. It is found that at the edge of the storms, electrons were depleted at the lower kilometers of the D-layer, and farther away from the storms, the electron profiles gradually changed to a normal background profile. However, directly above the storms, it was observed that the electron density can either be reduced or enhanced, depending on the electrical activity of the underlying storms.

**SPRT-07      Streamer Discharges from Dielectric Hydrometeors - by Samaneh Sadighi**

Status of First Author: Student IN poster competition, PhD

**Authors:** Samaneh Sadighi (ssadighi2009@my.fit.edu),  
Dr. Ningyu Liu (nliu@fit.edu)  
Dr. Joseph R. Dwyer (jdwyer@fit.edu)  
Dr. Hamid K. Rassoul (rassoul@fit.edu)

**Abstract:** Despite many theories for lightning initiation, the question of how lightning starts in the thundercloud still remains unanswered. One theory of lightning initiation from the standpoint of conventional breakdown theory was brought forward by scientists in the late 1960's [e.g., Dawson, JGR, 74 (28), 6859, 1969; Griffiths and Latham, Quart. J. Roy. Meteorol. Soc., 100, 163, 1974]. They hypothesized that breakdown occurs in the thundercloud in the vicinity of water/ice particles called hydrometeors, where the cloud electric field is enhanced. Similar small particles of meteoric origin in the mesosphere and lower ionosphere could also be a possible contributing source of sprite initiation (as suggested by Zabolotin et. al. [GRL, 28(13), 2593, 2001]).

In our previous studies thundercloud hydrometeors were modeled using a neutral plasma column. Our simulation results showed successful formation of streamers from the model hydrometeors in a uniform applied electric field below the conventional breakdown threshold field. One concern with using an ionization column is whether this patch of ionization is a proper representation of a dielectric hydrometeor. In the present study, we seek to address this concern. We have utilized the streamer discharge model developed by Liu and Pasko [JGR, 109, A04301, 2004] to tackle the streamer initiation problem. This plasma discharge model has been modified to accommodate a single isolated spherical dielectric inside the computational region. The governing equations are discretized on a Cartesian grid, which does not conform to the curvature of the dielectric hydrometeor. The two key aspects that need to be considered in this case are implementation of proper boundary conditions on the curved boundary and accurate representation of the discretized parameters of the governing equations in the cells that are cut by this boundary. A boundary-cut cell method developed by Ye et. al. [J. Comp. Phys., 156, 209, 1999] has been implemented to address these two issues for the cells cut by the sphere boundary. Initial modeling results from this study will be presented.

## **Stratosphere Studies and Below**

### **STRB-01      Production of very high potential in intra-cloud lightning in connection with terrestrial gamma ray flashes - by Sotirios A. Mallios**

Status of First Author: Student IN poster competition, PhD

**Authors:** Sotirios A. Mallios, Sebastien Celestin, and Victor P. Pasko

**Abstract:** High altitude positive intra-cloud (+IC) flashes (the negative lightning leader propagates up toward the positive charge region, while the positive leader propagates down to the negative charge region) in their development stage have been correlated with terrestrial gamma-ray flashes (TGFs) [Williams et al., J. Geophys. Res., 111, D16209, 2006; Stanley et al., Geophys. Res. Lett., 33, L06803, 2006]. TGFs are high energy photon bursts originating from the lower altitudes of the Earth's atmosphere due to the brehmsstrahlung emission by energetic electrons during the thunderstorm activity, which are observed by space-born detectors in low Earth orbit. Bidirectional leaders that initiate IC lightning discharges develop electric potential differences in the vicinity of their heads with respect to the ambient large scale potential. This process has been suggested to be of essential importance in TGFs [Celestin and Pasko, J. Geophys. Res., 116, A03315, 2011]. Using a 3-D cartesian fractal model, we quantify the electric potential produced in a developing +IC lightning for given thunderstorm electric configurations. In particular, this allows for determining the electric potential difference between the lightning leader and the large-scale thunderstorm potential in the region of the leader head. In the current work, we present the case of a +IC lightning network in a thunderstorm configuration that leads to a very high potential difference between the leader head and the ambient potential. We demonstrate that specific thundercloud configuration can create very high potential cases, and we show how a delay in the development of the negative leader can produce a high potential difference in the negative leader head region.

**STRB-02      A spatially scanning lower and middle atmospheric lidar system in northwest New Jersey - by Anthony Teti**

Status of First Author: Student IN poster competition, Masters

**Authors:** Anthony Teti at235@njit.edu  
Dr. Andrew J. Gerrard Gerrard@njit.edu

**Abstract:**

We present recent results from our middle and upper atmospheric lidar observatory located in northwest New Jersey. The lidar system currently uses a 4-W 532-nm laser system with a 4" Meade optical telescope to collect molecular and aerosol return from the troposphere and stratosphere. The system is used to measure a) lower and middle atmospheric gravity wave structures, b) lower atmospheric cloud/aerosol formations, and c) frontal systems as progenitors of gravity waves.

**STRB-03      Source Altitudes of Terrestrial Gamma-Ray Flashes Produced by Stepping Lightning Leaders - by Wei Xu**

Status of First Author: Student IN poster competition, PhD

**Authors:** Wei Xu, Sebastien Celestin and Victor P. Pasko

**Abstract:** Terrestrial Gamma-ray Flashes (TGFs) are high-energy photon bursts originating from the Earth's atmosphere. After their discovery in 1994 by the Burst and Transient Source Experiment (BATSE) detector aboard the Compton Gamma-Ray Observatory [Fishman et al., Science, 264, 1313, 1994], this phenomenon has been further observed by the Reuven Ramaty High Energy Solar Spectroscopic Imager (RHESSI) [Smith et al., Science, 307, 1085, 2005], the Fermi Gamma-ray Space Telescope [Briggs et al., JGR, 115, A07323, 2010] and the Astrorivelatore Gamma a Immagini Leggero (AGILE) satellite [Marisaldi et al., JGR, 115, A00E13, 2010]. Moreover, measurements have correlated TGFs with initial development stages of normal polarity intracloud lightning that transports negative charge upward (+IC) [e.g., Lu et al., GRL, 37, L11806, 2010; JGR, 116, A03316, 2011]. Photon spectra corresponding to well-established model of relativistic runaway electron avalanches (RREAs) usually provide a very good agreement with satellite observations [Dwyer and Smith, GRL, 32, L22804, 2005]. However, it has been suggested that long unbranched +IC lightning leaders could produce a sufficient number of energetic electrons to explain TGFs without invoking further amplification in RREAs [Celestin and Pasko, JGR, 116, A03315, 2011]. Besides, Tavani et al. [PRL, 106, 018501, 2011] have shown that a significant deviation from the RREA spectrum is present at high energy (>30 MeV). In this work, we use Monte Carlo models to study the photon spectra at low-orbit satellite altitudes associated with energetic electrons produced during the negative corona flashes of stepping negative leaders in +IC discharges. We show that the obtained spectra are consistent with current satellite measurements. This suggests that TGFs can be directly produced by lightning discharges. We show that the TGF spectrum produced by acceleration of electrons in the electric field of stepping IC leaders involves deeper source altitudes in the atmosphere.

Agner, Ryan, 10

Bartlett, Nate, 20

Bossert, Katrina, 15

Butterfield, Zachary, 14

Cai, Xuguang, 12

Chen, Cao, 13

Collins, Richard, 19

Conde, Mark, 2

Criddle, Neal, 11

Crowley, Geoff, 10

da Silva, Caitano, 24

Fletcher, Alex, 4

Fong, Weichun, 16

Greer, Katelynn, 21

Hall, Stephen, 3

Heale, Christopher, 9

Holt, Laura, 7

Hsu, Vicki, 4

Huang, Wentao, 16

Kavanagh, Andrew, 1

Kosar, Burcu, 25

Lay, Erin, 10

Lee, Nicolas, 4

Li, Zhenhua, 12

Lin, Cissi, 18

Liu, Ningyu, 24

Lu, Xian, 8

Mahmoudian, Alireza, 1

Mallios, Sotirios, 27

Mangogna, Tony, 12

Marshall, Robert, 13

Martus, Cameron, 15

Matthias, Vivien, 22

Mesquita, Rafael, 6

Mitchell, Michael, 20

Moore, Robert, 25

Negale, Michael, 11

Nguyen, Vu, 23

Pedatella, Nicholas, 21

Pifko, Steven, 7

Placke, Manja, 8

Qin, Jianqi, 26

Roberts, Brenden, 19

Sadighi, Samaneh, 26

Saran, Deepali, 18

Sassi, Fabrizio, 24

Shao, Xuan-Min, 26

She, Chiao-Yao, 22

Sousa, Austin, 6

Sox, Leda, 17

Stephens, Zachary, 6

Takahashi, Toru, 14

Teti, Anthony, 28

Vadas, Sharon, 9

Vaudrin, Cody, 3

Volz, Ryan, 5

Westerhoff, John, 16

Wu, Qian, 23

Xu, Wei, 28

Yee, Jonathan, 5

Yonker, Justin, 17

Yu, Zhibin, 15

Zhu, Qian, 6